Report 2798

NAVAL SHIP RESEARCH AND DEVELOPMENT CENTER
Washington, D.C. 20007

COMPUTATIONAL METHOD FOR DETERMINATION OF BUBBLE DISTRIBUTIONS IN LIQUIDS (U)

by

Terry Brockett

HYDROMECHANICS LABORATORY
RESEARCH AND DEVELOPMENT REPORT

April 1969

Report 2798

COMPUTATIONAL METHOD FOR DETERMINATION OF BUBBLE DISTRIBUTIONS IN LIQUIDS (U)

The Naval Ship Research and Development Center is a U.S. Navy center for laboratory effort directed at achieving improved sea and air vehicles. It was formed in March 1967 by merging the David Taylor Model Basin at Carderock, Maryland and the Marine Engineering Laboratory at Annapolis, Maryland. The Mine Defense Laboratory, Panama City, Florida became part of the Center in November 1967.

Naval Ship Research and Development Center
Washington, D.C. 20007

NDW-NSRDC 3960/43 (10-67)

DEPARTMENT OF THE NAVY
NAVAL SHIP RESEARCH AND DEVELOPMENT CENTER
WASHINGTON, D. C. 20007

COMPUTATIONAL METHOD FOR DETERMINATION OF BUBBLE DISTRIBUTIONS IN LIQUIDS (U)

by

Terry Brockett

April 1969

Report 2798

TABLE OF CONTENTS

LIST OF FIGURES

NOTATION

A	Term appearing in the summation for the real component of compressibility, introduced in Equation [43]
A_o	Amplitude of spherical wave, introduced in Equation [18]
a	Real part of complex compressibility, introduced in Equation [26]
B	Term appearing in the summation for the imaginary component of compressibility, introduced in Equation [44]
b	Imaginary portion of complex compressibility, introduced in Equation [26]
C	Velocity of propagation for a sound wave in the bubbly water, introduced in Equation [19]
C_o	Velocity of propagation in bubble-free water
D	Generalized damping function, introduced in Equation [7]
I_n	Integral appearing in the expression for the complex compressibility, introduced in Equation [39]
K	Complex compressibility, introduced in Equation [18], defined in Equation [31]
m	Subscript of band interval for which attenuation is sought, introduced in Equation [49]
N	Number of intervals or bands into which data is resolved, introduced in Equation [39]
n	Subscript for summation, introduced in Equation [39]
P	Amplitude of term in Fourier series of pressure wave, introduced in Equation [11]
p	Sound pressure at a distance r from the source, introduced in Equation [18]
P_g	Pressure due to gas inside a bubble, introduced in Equation [1]
P_v	Vapor pressure of liquid, introduced in Equation [1]
P_∞	Pressure far from the bubble, introduced in Equation [16]
R	Instantaneous bubble radius, introduced in Equation [5]
R_o	Equilibrium bubble radius, introduced in Equation [1]
r	Distance from sound source, introduced in Equation [18]
r_o	Reference distance from sound source, introduced in Equation [18]
α	Attenuation of sound, introduced in Equation [19]

γ Ratio of specific heats for a gas, adiabatic expansion constant, introduced in Equation [2]

δ Resonant damping constant for small bubble motions, introduced in Equation [16]

ε Nondimensional half interval of band, introduced in Equation [39]

η Polytropic expansion coefficient for the gas, introduced in Equation [2]

ν Concentration of gas per unit volume of mixture, introduced in Equation [34]

ρ Density of water, introduced in Equation [6]

σ Surface tension of liquid gas interface, introduced in Equation [1]

τ Concentration function, introduced in Equation [36]

ω Driving frequency, introduced in Equation [11]

ω_o Resonant frequency for bubble of radius R_o, introduced in Equation [13]

ABSTRACT

An analytical method of determining the gas bubble spectrum in a liquid from the measured acoustic attenuation is examined. The analysis is based on the linearized equations of motion for a spherical bubble with damping. The bubbles are assumed to be homogeneously distributed in the liquid and the bubble concentration and damping are assumed constant in a small size interval. The acoustic wavelength is assumed much greater than the bubble dimensions and bubbles are assumed far enough apart that no interactions occur. The direct solution gives the acoustic attenuation of a known bubble distribution at any given frequency. An iteration procedure is incorporated in a FORTRAN program for converting acoustic attenuation as a function of frequency to bubble concentration as a function of size. For air bubbles in water, the effects of physical properties on the bubble spectrum are examined with the computer program. Experiments in the 12-inch water tunnel are described.

ADMINISTRATIVE INFORMATION

NSRDC internal funding from the General Hydrodynamic Research Program supported this work under Subproject S-R009 01 01, Task 0101, Problem 526-355.

INTRODUCTION

Cavitation in a liquid occurs when the pressure reaches values that are low enough to rupture the media at certain weak spots or nuclei sites. At the pressures for which cavitation occurs in practical situations, several possible rupture sites have been proposed: free gas bubbles in the liquid, gas bubbles on the surface of a solid immersed in the liquid, gas nucleation sites in cracks or pores in the surface of the solid, and the strength of the molecular bond between liquid and solid.[1*] Of these, the gas bubbles in the liquid and the gas nucleation sites on the surface of the solid are presently receiving most attention in investigations of hydrodynamic cavitation.[2,3,4] One of the two sites for gas nuclei, the free stream bubbles, is a function of only the environment. Thus, a reasonable

---

*References are listed on page 59.

starting place to evaluate model/full-scale extrapolation would be to compare gas nuclei in both systems. However, to date no demonstration has clearly established that gas bubbles in the stream are more important than any of the other proposed nuclei sites.

Although the need for, and some of the problems associated with, detection of bubbles in liquids has been recognized, there is as yet no entirely satisfactory method of detecting bubble distributions. The two most promising approaches to the problem are optic and acoustic. The optical method involves either scattering measurements[5] from a region containing bubbles or detection of properties of a single bubble such as the individual diffraction pattern[6] or direct photograph.[7,8] The scattering experiments are not satisfactory since there is not sufficient variation as a function of scattering angle.[5] Examination of a single bubble is a complex problem* and usually involves high-speed equipment and a good light source such as a laser. Such equipment would be difficult to move and realign from one place to another and evaluation of a bubble distribution would be time consuming.

Detection of bubbles by optical means requires the use of complex equipment, but acoustic detection based on transmission of sound through the liquid can be accomplished with standard laboratory equipment. Usually one of two approaches is considered, both based on amplitude attenuation. In small closed vessels, reverberation decay is generally used.[5,9] For larger vessels with high attenuation (due to the large number of bubbles present), such a method would not work. In a large volume of liquid, transmission across a known path length is used.[10,11,12] The significant variable in this case is attenuation per unit length.

To date, the only successful bubble distribution measurement in a moving liquid is that accomplished by Ripkin and Killen[12] with the acoustic method. Their analysis was derived from relations for transmission through a water-bubble mixture developed by Meyer and Skudrzyk.[13] (Other

---

*However, following a single bubble would be an excellent means of evaluating the processes involved as a bubble flows from the stream into a cavitation zone.

investigations of the acoustic effects of bubbles are discussed in References 14-17.) The attenuation per unit length is measured at specified frequency intervals over a suitably large range of frequencies, preferably over a large enough range so that there is no excess attenuation at either end. The analysis of Meyer and Skudrzyk[13] is reanalyzed to convert these data to the volume concentration at various radii. The instrumentation as used by them is limited at high frequencies (small bubbles) by the transducer characteristics and at low frequencies (large bubbles) by the environmental configuration.

The work at this Center was originally intended to duplicate as closely as possible the setup of Ripkin and Killen[12] for use in the water tunnels. It was soon obvious that in addition to the typographical errors in the analytical section of their report, there were also assumptions that had not been clearly stated in the development. Thus the present work was undertaken to show explicitly the assumptions made and to examine the analysis.

In the following work, the necessary equations are first derived in terms of propagation across a bubble-liquid mixture. Then the iteration scheme is described for resolving the measured transmission properties into the bubble distribution. Next, the computer program for data analysis is discussed and, using it, typical input is examined to provide a guide in the point spacing and accuracy of the experimental data. Finally, the method of analysis is discussed and attention is called to areas needing further investigation.

Appendix A presents equations for calculating bubble damping, Appendix B lists the FORTRAN statements of the computer program, and Appendix C gives details of attenuation-measurements in the NSRDC 12-in. water tunnel.

ANALYSIS OF BUBBLE MOTION

Spherical bubbles are assumed to enter the sound field in static equilibrium and the sound pressure is assumed to be the only forcing function acting on them. The attenuation of a bubble distribution is calculated on the basis of the response of a single bubble to the driving pressure. Experimentally the attenuation is measured so the analysis must be inverted to give the bubble concentration as a function of the measurements. The inversion is accomplished by iteration.

The development is limited to bubbles which are small relative to the acoustic wavelength so that the pressure on a bubble is a function of only time and not space. Also the medium is treated as a uniform mixture without point to point variations. Bubbles gradually encounter the measuring pressure wave since the attenuation is large. Any transient effects of the encounter are assumed to be negligible or to have died out by the time the bubbles produce attenuation in the measured path length.

STATIC CASE

Far from the measuring apparatus, the bubbles are assumed to be in static equilibrium. The pressure inside and the pressure outside differ because of the surface tension.

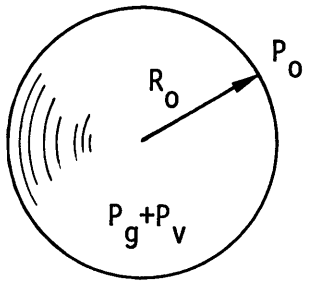

Figure 1 - Bubble Schematic

A static balance across the bubble wall relates the pressure outside to the internal pressure by

$$P_o = P_g + P_v - 2\frac{\sigma}{R_o} \qquad [1]$$

where P_o is the static pressure immediately outside the wall,
P_g is the gas pressure inside the bubble,
P_v is the vapor pressure of the surrounding liquid,
σ is the surface tension coefficient, and
R_o is the bubble radius.

Note that the pressure inside ($P_g + P_v$) is greater than the pressure outside (P_o).

The amount of gas within the bubble is assumed to remain constant (i.e., negligible diffusion). The relationship between pressure and volume is given by

$$P_g \left(4 \pi \frac{R_o^3}{3}\right)^{\eta} = \text{constant} \qquad [2]$$

where η is the polytropic expansion constant,* $1 < \eta < \gamma$, and

γ is the adiabatic expansion constant and equal to the specific heat ratio.

Thus

$$P_g = \frac{\text{constant}}{R_o^{3\eta}} \qquad [3]$$

and

$$P_o = P + \frac{\text{constant}}{R_o^{3\eta}} - \frac{2\sigma}{R_o} \qquad [4]$$

LINEARIZED MOTION OF A SINGLE BUBBLE

When dynamic movement occurs, the pressure differences across the wall of the bubble is still controlled by the surface tension effect as determined by static analysis, and the internal gas continues to follow the pressure-volume relationship in Equation [3]. Thus, the pressure outside the bubble undergoing forced motion is

$$P(R) = P_v + \left[P_o - P_v + \frac{2\sigma}{R_o}\right] \left(\frac{R_o}{R}\right)^{3\eta} - 2\frac{\sigma}{R} \qquad [5]$$

where P(R) is the pressure outside the bubble wall, and R is the instantaneous bubble radius. The other symbols are as previously defined and now denote reference conditions.

---

*Large bubbles expand and contract adiabatically (i.e., $\eta = \gamma$) and small bubbles vibrate isothermally (i.e., $\eta = 1$). The Devin survey[18] gives expressions for calculating η (see Appendix A).

When there is no damping, the nonlinear equation of motion of a spherical bubble of radius R is given by[19]

$$R\ddot{R} + 3/2\ \dot{R}^2 = \frac{P(R) - P_\infty(t)}{\rho} \qquad [6]$$

where ρ is the density of the liquid,
$P_\infty(t)$ is the pressure far from the bubble, and the
dots denote differentiation with respect to time.

A damping term is added to this equation to give

$$R\ddot{R} + D\ (R,\dot{R})\ \dot{R} + 3/2\ \dot{R}^2 - \frac{1}{\rho}\left[P_o - P_v + \frac{2\sigma}{R_o}\right]\left(\frac{R_o}{R}\right)^{3\eta} + \frac{2\sigma}{\rho R} = \frac{P_v - P_\infty(t)}{\rho} \qquad [7]$$

where $D(R,\dot{R})$ is a generalized damping function.
For motion initiated by acoustic pressure signals,

$$R = R_o + \Delta R(t) \qquad [8]$$

where R_o is the equilibrium bubble radius and $(\Delta R)^\ell$, $\ell \geq 2$ is negligible as well as any differentials involving $(\Delta R)^\ell$.

The linearized equation of motion becomes

$$R_o\ \Delta\ddot{R} + D_o(R_o)\ \Delta\dot{R} + \frac{3\eta}{\rho R_o}\left[P_o - P_v + \frac{2\sigma}{R_o}\left(1 - \frac{1}{3\eta}\right)\right]\ \Delta R = \frac{P_o - P_\infty(t)}{\rho} \qquad [9]$$

This equation is an ordinary, linear second-order differential equation for ΔR as a function of time. Since the equation is linear, only one component of the Fourier series used to represent any pressure wave need be considered.

The pressure many diameters from the bubble, $P_\infty(t)$, will consist of the undisturbed pressure plus the acoustic pressure wave:

$$P_\infty(t) = P_o + \sum_{q=1}^{\infty} P_q \exp(i\omega_q t) \qquad [10]$$

where P_o is the undisturbed pressure,

P_q is an amplitude term, independent of time,

ω_q is the qth radial frequency ($\omega_q = q\omega_1$), and

ω_1 is the repetition frequency of acoustic pressure wave.

With only one of the harmonic terms in the driving pressure,

$$P_\infty(t) = P_o + P \exp(i\omega t) \qquad [11]$$

The equation of motion becomes therefore

$$\ddot{\Delta R} + \frac{D_o(R_o)}{R_o}\dot{\Delta R} + \frac{3\eta(P_o - P_v)}{\rho R_o^2}\left[1 + \frac{2\sigma}{R_o(P_o - P_v)}\left(1 - \frac{1}{3\eta}\right)\right]\Delta R = -\frac{1}{\rho R_o} P \exp(i\omega t) \qquad [12]$$

The natural, or resonant, frequency is obtained from this equation when there is no driving function (i.e., P = 0). When the driving force is zero, the frequency of oscillations can be found by assuming a solution $\Delta R = A \exp(i\omega_o t)$ where ω_o is the resonant frequency. This gives

$$\omega_o = \sqrt{\frac{3\eta(P_o - P_v)}{\rho R_o^2}\left[1 + \frac{2\sigma(1 - \frac{1}{3\eta})}{R_o(P_o - P_v)}\right] - \left[\frac{D_o(R_o)}{2 R_o}\right]^2} \qquad [13]$$

Since the damping is small, it can be ignored in the above expression to give

$$\omega_o R_o = \sqrt{\frac{3\eta(P_o - P_v)}{\rho}\left[1 + \frac{2\sigma(1 - \frac{1}{3\eta})}{R_o(P_o - P_v)}\right]} \qquad [14]$$

Figure 2 is a graph of this equation. In some cases, the surface tension effect will be small and the resonant frequency becomes simply

$$\omega_o R_o = \sqrt{\frac{3\eta(P_o - P_v)}{\rho}} = \text{constant}$$

Alternatively, this can be considered as the first approximation to the bubble size whose resonant frequency is known.

The solution for forced motions with damping, responding to the driving pressure $P_\infty(t)$ in Equation [11], is readily found to be

$$\Delta R = \frac{-P \exp(i\omega t)}{\omega^2 R_o \rho \left\{ \frac{3\eta(P_o - P_v)}{\omega^2 \rho R_o^2} \left[1 + \frac{\left(2\sigma\ 1 - \frac{1}{3\eta}\right)}{R_o(P_o - P_v)} \right] - 1 + \frac{D_o(R_o)}{\omega R_o} \right\}}$$

and with Equation [14],

$$\Delta R = \frac{-P \exp(i\omega t)}{\omega^2 R_o \rho \left\{ \left(\frac{\omega_o}{\omega}\right)^2 - 1 + \frac{D_o(R_o)}{\omega R_o} \right\}} \qquad [15]$$

The damping constant is calculated from the equations compiled by Devin.[18] His damping constant δ is related to D_o by

$$\delta = \frac{D_o}{\omega_o R_o} \qquad [16]$$

The effect of damping* is small except near resonance. Calculations to be discussed later show that some margin can be tolerated in the value of the damping; thus it is permissible to take $\omega_o R_o$ constant in Equation [16] so that the new damping constant is, in fact, still constant. With δ as the damping constant, the equation for ΔR becomes

$$\Delta R = \frac{-P \exp(i\omega t)}{\omega^2 R_o \rho \left\{ \left(\frac{\omega_o}{\omega}\right)^2 - 1 + i \frac{\omega_o}{\omega} \delta \right\}} \qquad [17]$$

---

*The damping of bubbles arises from three sources: thermal absorption, reradiation, and viscous dissipation. Although the damping constant is also a function of driving frequency, its value here is taken as that at resonance since for small damping its major effect is confined to a region near resonance.

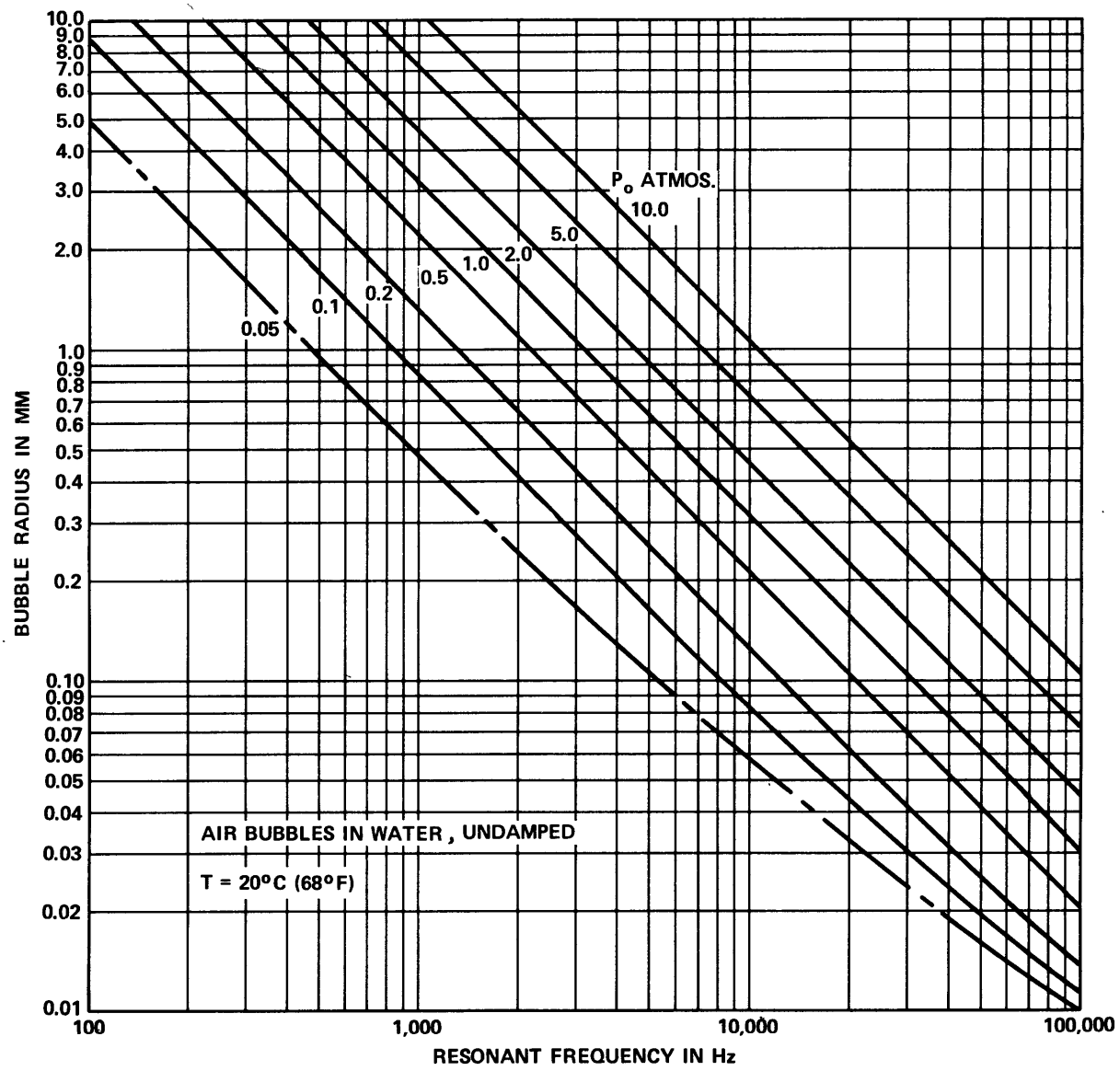

Figure 2 - Resonant Frequency of Air Bubbles in Water

PROPAGATION OF ATTENUATED ACOUSTIC SIGNALS

It is assumed that in most applications, sound waves will be radiated into the bubbly mixture by a transducer which is small relative to the wavelength of the driving frequency. When these conditions hold, the wave forms can be considered as diverging spherical waves.

The solution to the wave equation for a harmonically vibrating spherical wave transmitting in a homogeneous medium of uniform density is conveniently expressed as

$$p = \frac{A_o}{r} \exp\left\{i\omega\left[t - \sqrt{\rho K}(r - r_o)\right]\right\} \qquad [18]$$

where

p is the instantaneous pressure at a distance r from the source,
A_o is a complex constant,
ω is the driving frequency,
K is the compressibility (see below),
r is the distance from source to receiver, and
r_o is the reference distance.

Attenuation occurs when the compressibility K is complex:

$$\sqrt{\rho K(\omega)} = \frac{1}{C} + \frac{i}{\omega}\alpha(\omega)$$

$$= \frac{1}{C_o + \Delta C(\omega)} + \frac{i}{\omega}\left[\alpha_o(\omega) + \alpha_\beta(\omega)\right] \qquad [19]$$

where

$C = C_o + \Delta C(\omega)$ is the velocity of propagation of the ω frequency component, i.e., phase velocity;
C_o is the velocity in the liquid alone;
$\Delta C_o(\omega)$ is the increment of velocity arising from the bubbles;

$\alpha(\omega) = \alpha_o(\omega) + \alpha_\beta(\omega)$ is the attenuation per unit length at the frequency ω;

$\alpha_o(\omega)$ is the attenuation in the liquid alone, usually negligible in water; and

$\alpha_\beta(\omega)$ is the additional attenuation produced by the bubbles.

The acoustic pressure is

$$p = \frac{A_o}{r} \exp\left\{ i\omega \left[t - \frac{(r - r_o)}{c} \right] \right\} \exp\left[\alpha(r - r_o) \right] \qquad [20]$$

To determine the presence of bubbles, identical sound waves are sent into the liquid with and without bubbles (e.g., in a water tunnel, this could be the test conditions and then the test conditions except with a high static pressure).

Let $p_{w/out}$ be the signal received at r_1 when there are no bubbles present:

$$p_{w/out} = \frac{A_o}{r_1} \exp\left\{ i\omega \left[t - (r_1 - r_o)/C_o \right] \right\} \exp\left[\alpha_o (r_1 - r_o) \right]$$

and when there are bubbles present, the sound received is $p_{w/}$,

$$p_{w/} = \frac{A_o}{r_1} \exp\left\{ i\omega \left[t - (r_1 - r_o)/C \right] \right\} \exp\left\{ (\alpha_o + \alpha_B)\ (r_1 - r_o) \right\}$$

The ratio of those two signals is then:

$$\frac{p_{w/}}{p_{w/out}} = \exp\left[i\omega (r_1 - r_o) \left(\frac{1}{C_o} - \frac{1}{C_o + \Delta C} \right) \right] \exp\left[\alpha_B (r_1 - r_o) \right] \qquad [21]$$

The small concentrations of bubbles expected in most situations (volume concentration $\sim 10^5$) have little effect on the speed of sound but a large effect on attenuation. Since the velocities are nearly the same, their difference is small and the propagation of sound through a bubbly

liquid is characterized by the attenuation and is approximately*

$$\frac{p_{w/}}{p_{w/out}} = \exp\left[\alpha_\beta\ (r_1 - r_o)\right] \qquad [22]$$

Hence the attenuation is:

$$\alpha_\beta = -\left(\frac{1}{r_1 - r_o}\right) \ell n \left(\frac{p_{w/out}}{p_{w/}}\right) \qquad [23]$$

where the units would be nepers per unit length. The above expression would be convenient when pressures are measured at the two conditions. In some cases, an attenuation box (calibrated in decibels) would be used to compare the signals for which $20 \log_{10} p_{w/out}/p_{w/}$ (i.e., decibels) is read on a scale. Then

$$-\left(20 \log_{10} \frac{p_{w/out}}{p_{w/}}\right) = 8.686\ \alpha_\beta\ (r_1 - r_o) \qquad [24]$$

where α_β is still in nepers per unit length. Since 8.686 converts from nepers to decibels, the attenuation in the more common decibels would be

$$8.686\ \alpha_\beta = \text{attenuation in decibels per unit length}$$

$$= -\frac{20 \log_{10} \frac{p_{w/out}}{p_{w/}}}{r_1 - r_o} \qquad [25]$$

In the following work, the conversion of nepers to decibels is a needless bother and the attenuation is expressed in nepers per unit length.

To relate the velocity and attenuation to the components of the complex compressibility, it is convenient to put

$$K = a + i\ b \qquad [26]$$

---

*Obviously where attenuation is a small fraction of the peak value and velocity far from the pure water value, e.g., low frequencies, this approximation might not be valid. Other experimental methods[8,10,13] might be considered if this becomes a problem.

where a and b are real, and, as will be shown for typical cases with small concentrations of bubbles, $|a| > |b|$, $a > 0$, $b < 0$. To find the velocity and attenuation the square root in Equation [19] must be obtained. The square root with a positive velocity is the one sought, which gives

$$\sqrt{\rho K} = \sqrt{\frac{\rho}{2}\left(\sqrt{a^2 + b^2} + a\right)} - i\sqrt{\frac{\rho}{2}\left(\sqrt{a^2 + b^2} - a\right)} \qquad [27]$$

Therefore

$$c = \frac{1}{\sqrt{\frac{\rho}{2}\left(\sqrt{a^2 + b^2} + a\right)}}$$

$$= \sqrt{\frac{2}{\rho}}\sqrt{\sqrt{a^2 + b^2} - a}\Big/|b| \qquad [28]$$

$$\frac{\alpha}{\omega} = -\sqrt{\frac{\rho}{2}\left(\sqrt{a^2 + b^2} - a\right)} = -\frac{\rho}{2} c\,|b|$$

$$= \frac{\rho}{2} cb \qquad [29]$$

Calculations show that the velocity for small concentrations is close to the bubble-free value. The expression for velocity may then be approximated:

$$c \approx \sqrt{\frac{2a}{\rho}} \frac{\sqrt{1 + 1/2\,\frac{b^2}{a^2} - 1}}{|b|} = \sqrt{\frac{1}{\rho a}} \qquad [30]$$

COMPUTATION OF COMPRESSIBILITY

To determine the value of the compressibility from the bubble motion, the definition relating deformation to applied stress is used. For transmission of sound, the compressibility is defined as

$$K = -\frac{\Delta v}{V \Delta p} \qquad [31]$$

where V is the total volume acted upon,

Δp is the change in pressure,

$\Delta p = P\exp(i\omega t)$ from Equation [11], and

Δv is the change in volume resulting from the pressure change from Equation [17].

The minus sign is needed since the pressure and volume changes are 180 deg out of phase with each other. The compressibility will be that associated with the liquid alone plus the contribution from the bubbles; that is, the change in volumes per unit change in pressure ($\Delta v/\Delta p$) will be additive since the additional volume of bubbles is negligible in the total volume.

For bubble-free liquid, the following relation holds from Equation [19]

$$K = \frac{1}{\rho C_o^2} - \frac{\alpha_o^2}{\omega^2 \rho} - i\frac{2\alpha_o}{\rho C_o \omega} \qquad [32]$$

Based on an equation[20] for attenuation of water alone, the real part of K is dominated by the velocity term at frequencies below 10^{11} Hz. Thus the pure water compressibility can be taken as

$$K = \frac{1}{\rho C_o^2} - i\frac{2\alpha_o}{\rho C_o \omega} \qquad [33]$$

To evaluate the compressibility, the change in volume for the bubble must be computed. If the bubbles were all of the same size, the total volume change would be simply the number of bubbles times the volume change for a single bubble. For a mixture of bubble sizes, a concentration is used so that the number of bubbles of radius R_o per unit volume of mixture is

$$\frac{\text{number of bubbles}}{V} = \frac{d\nu\,(R_o)}{4/3\,\pi\,R_o^3} \qquad [34]$$

where $d\nu$ is the elemental volume concentration per unit volume for bubbles of radius R_o.

The total volume change per unit volume for the bubble is now

$$\frac{\Delta v}{V} = \int_{R_{oMin}}^{R_{oMax}} 4\pi R_o^2 \Delta R \frac{d\nu(R_o)}{4/3\pi R_o^3} = 3\int_{R_{oMin}}^{R_{oMax}} \frac{\Delta R}{R_o} d\nu(R_o) \qquad [35]$$

The elemental volume concentration can be taken either as a function of equilibrium size (i.e., radius) or as a function of resonant frequency. The following development will be based on the concentration as a function of resonant frequency. Since concentration is a function of natural frequency, let

$$d\nu(R_o) = \frac{1}{2\pi} \tau(\omega_o) d\omega_o \qquad [36]$$

So that the total concentration is

$$\nu = \frac{1}{2\pi} \int_o^\infty \tau(\omega_o) d\omega_o \qquad [37]$$

where τ is a concentration function.

From Equation [17], the compressibility becomes

$$K(\omega) = \frac{1}{\rho C_o^2} - i\frac{2\alpha_o}{\rho C_o \omega} + \frac{3}{2\pi\rho\omega^2} \int_{\omega_{oMin}}^{\omega_{oMax}} \frac{\omega_o^2 \tau(\omega_o) d\omega_o}{(\omega_o R_o)^2 \left\{ \left(\frac{\omega_o}{\omega}\right)^2 - 1 + i\frac{\omega_o}{\omega}\delta \right\}}$$

where ω_{oMin} and ω_{oMax} are the resonant frequencies for the smallest and largest bubbles present. In practice, this will correspond to the upper and lower frequencies for which significant attenuations as defined by Equation [25] can be determined.

Let $Z = \frac{\omega_o}{\omega}$ and obtain

$$K(\omega) = \frac{1}{\rho C_o^2} - i\frac{2\alpha_o}{\rho C_o \omega} + \frac{\omega}{2\pi\,(P_o - P_v)} \int_{Z_{Min}}^{Z_{Max}} \frac{1}{\eta\left[1+\frac{2\sigma\left(1-\frac{1}{3\eta}\right)}{R_o\left(P_o - P_v\right)}\right]} \times \frac{Z^2\,\tau(Z)\,dZ}{Z^2 - 1 + i\,Z\,\delta(Z)} \qquad [38]$$

where Z_{Min} corresponds to the lowest resonant frequency present and Z_{Max} to the highest. The above equation is essentially Equation [22] in Meyer and Skudrzyk.[13]

To perform the integration, the concentration function $\tau(Z)$ is approximated by a series of steps in which $\tau_n(Z)$ is constant. In addition, all slowly varying quantities (i.e., η, δ, and $[1 + 2\sigma/R_o(P_o - P_v)\,(1 - 1/3\eta)]$) are also taken as constant with their value that at midband. The compressibility then becomes

$$K(\omega) = \frac{1}{\rho C_o^2} - i\frac{2\alpha_o}{\rho C_o \omega} + \frac{\omega}{2\pi\left(P_o - P_v\right)} \sum_{n=1}^{N} \frac{\tau_n\, I_n(\omega)}{\eta_n\left[1+\frac{2\sigma\left(1-\frac{1}{3\eta_n}\right)}{R_{o_n}\left(P_o - P_v\right)}\right]} \qquad [39]$$

where $I_n(\omega) = \int_{Z_n-\varepsilon_n}^{Z_n+\varepsilon_n} \frac{Z^2\,dZ}{Z^2 - 1 + iZ\delta_n}$

N is the number of steps in the approximation of τ,

$\varepsilon_n = \frac{\Delta\omega_{o_n}}{2\omega}$ is the half interval for which τ_n and δ_n are taken constant,*

$Z_n = \frac{\omega_{o_n}}{\omega}$ is the value of Z at midband, and

$$\Delta\omega_{o_n} = \omega_{o_{n+1}} - \omega_{o_n}.$$

The integration involved in I can be performed to give

$$I_n(\omega) = \left[Z + \frac{\delta_n}{2} \tan^{-1} \frac{\delta_n Z}{Z^2-1} + \frac{2-\delta_n^2}{4\sqrt{4-\delta_n^2}} \ln \frac{Z^2 - Z\sqrt{4-\delta_n^2}+1}{Z^2+Z\sqrt{4-\delta_n^2}+1} \right]_{Z_n-\varepsilon_n}^{Z_n+\varepsilon_n}$$

$$- i\left[\frac{2-\delta_n^2}{2\sqrt{4-\delta_n^2}} \tan^{-1} \frac{2\left(Z^2-1\right)+\delta_n^2}{\delta_n\sqrt{4-\delta_n^2}} + \frac{\delta_n}{4} \ln \left\{ \left(Z^2-1\right)^2 + \delta_n^2 Z^2 \right\} \right]_{Z_n-\varepsilon_n}^{Z_n+\varepsilon_n} \quad [40]$$

Figure 3 is a graph of I_n as a function of $1/Z = \omega/\omega_o$ for $\varepsilon_n = 1/8\ Z_n$. Thus the real and imaginary components of K in Equation [26] are

*The geometric mean rather than the arithmetic mean is generally used for the center frequency. For the results shown later in Figures 5 and 9, comparative calculations using the geometric center frequency differed by less than one percent except for the high frequency bands in the bubble distribution calculations. This is due mostly to changes in the band attenuation from the different averaging.

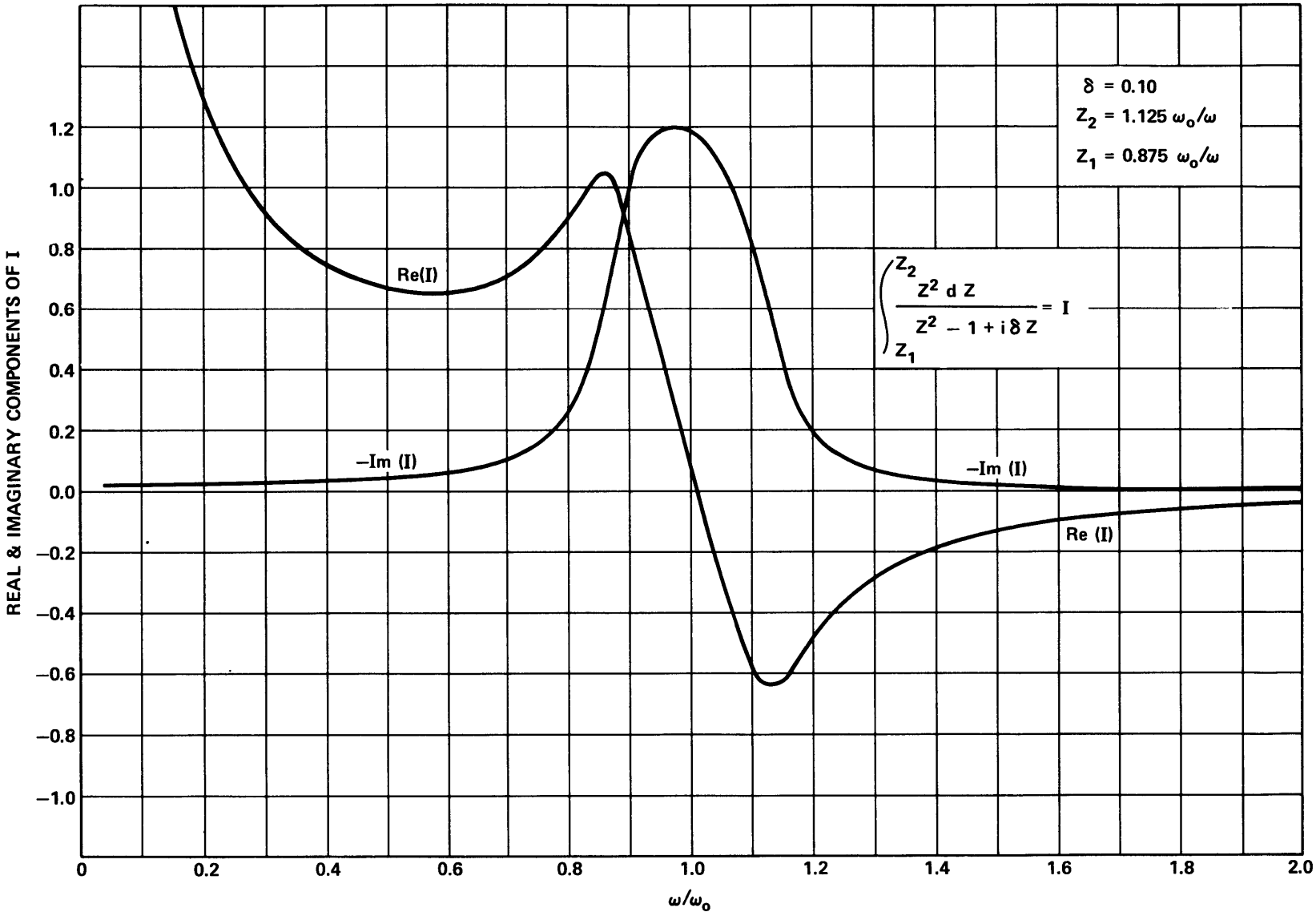

Figure 3 - Typical Components of Compressibility Integral

$$a(\omega) = \frac{1}{\rho C_o^2} + \frac{\omega}{2\pi(P_o - P_v)\gamma}\sum_{n=1}^{N}\tau_n \frac{\left[Z + \frac{\delta_n}{2}\tan^{-1}\frac{\delta_n Z}{Z^2-1} + \frac{2-\delta_n^2}{4\sqrt{4-\delta_n^2}}\ln\frac{Z^2 - Z\sqrt{4-\delta_n^2}+1}{Z^2+Z\sqrt{4-\delta_n^2}+1}\right]_{Z_n-\varepsilon_n}^{Z_n+\varepsilon_n}}{\frac{\eta_n}{\gamma}\left[1 + \frac{2\sigma\left(1 - \frac{1}{3\eta_n}\right)}{R_{o_n}(P_o - P_v)}\right]} \qquad [41]$$

and

$$-b(\omega) = 2\frac{\alpha_o}{\rho C_o \omega} + \frac{\omega}{2\pi(P_o - P_v)\gamma}\sum_{n=1}^{N}\tau_n \frac{\left[\frac{2-\delta_n^2}{2\sqrt{4-\delta_n^2}}\tan^{-1}\frac{2(Z^2-1)+\delta_n^2}{\delta_n\sqrt{4-\delta_n^2}} + \frac{\delta_n}{4}\ln\left\{(Z^2-1)^2 + \delta_n^2 Z^2\right\}\right]_{Z_n-\varepsilon_n}^{Z_n+\varepsilon_n}}{\frac{\eta_n}{\gamma}\left[1 + \frac{2\sigma\left(1 - \frac{1}{3\eta_n}\right)}{R_{o_n}(P_o - P_v)}\right]} \qquad [42]$$

Let the above expressions be

$$a(\omega) = \frac{1}{\rho C_o^2} + \frac{\omega}{2\pi(P_o - P_v)\gamma}\sum_{n=1}^{N}\tau_n A_n \qquad [43]$$

$$-b(\omega) = \frac{2\alpha_o}{\rho C_o \omega} + \frac{\omega}{2\pi(P_o - P_v)\gamma}\sum_{n=1}^{N}\tau_n B_n \qquad [44]$$

Generally the pure water attenuation will contribute little to the expression

for b and it can be ignored. Since both η and $1 + 2\sigma(1 - 1/3\eta)/[R_o(P_o-P_v)]$ are fixed at the midband value, variations in A and B are determined by variations in I. Equations [43] and [44] are now in a form where they can be directly substituted into Equations [28] and [29] to obtain the speed of sound and attenuation as a function of frequency in the bubble-liquid mixture with a known bubble distribution.

The calculations for attenuation involve the imaginary component of $I_n(\omega)$. Since I depends only on the bandwidth and damping constant, several values of each were used to calculate the imaginary component; see Figure 4. Calculations show that the peak value (near resonance) of the function varies slowly with damping when the bandwidth is held constant. The expected broadening occurs when the bandwidth is increased. The figure shows that the curves peak near resonance and that the contribution to the summation in neighboring bands is greater for frequencies below resonance than above it and less for large bandwidths than for small ones. The attenuation is proportional to the frequency squared times the imaginary component of $I_n(\omega)$, and hence the attenuation is higher above resonance than below for equal fractions of the center frequency from the resonant frequency. Increasing the damping constant is seen to increase the attenuation at off-resonance frequencies but to lower the value at resonance. The value of 0.2 for the damping constant in Figure 4 is the highest measured value for air bubbles in water.[14,15]

When the driving frequency ω is much lower than any resonant frequency ω_o, $Z >> 1$, and the function A_n becomes in the limit of large Z,

$$A_n \sim \frac{2\varepsilon_n + \frac{\delta_n}{2}\tan^{-1}\left[\delta_n\left(\frac{1}{Z_n+\varepsilon_n} - \frac{1}{Z_n-\varepsilon_n}\right)\right] + \frac{2-\delta_n^2}{4\sqrt{4-\delta_n^2}}\ln(1)}{\frac{\eta_n}{\gamma}\left[1 - \frac{2\sigma\left(1 - \frac{1}{3\eta_n}\right)}{R_{o_n}\left(P_o - P_v\right)}\right]}$$

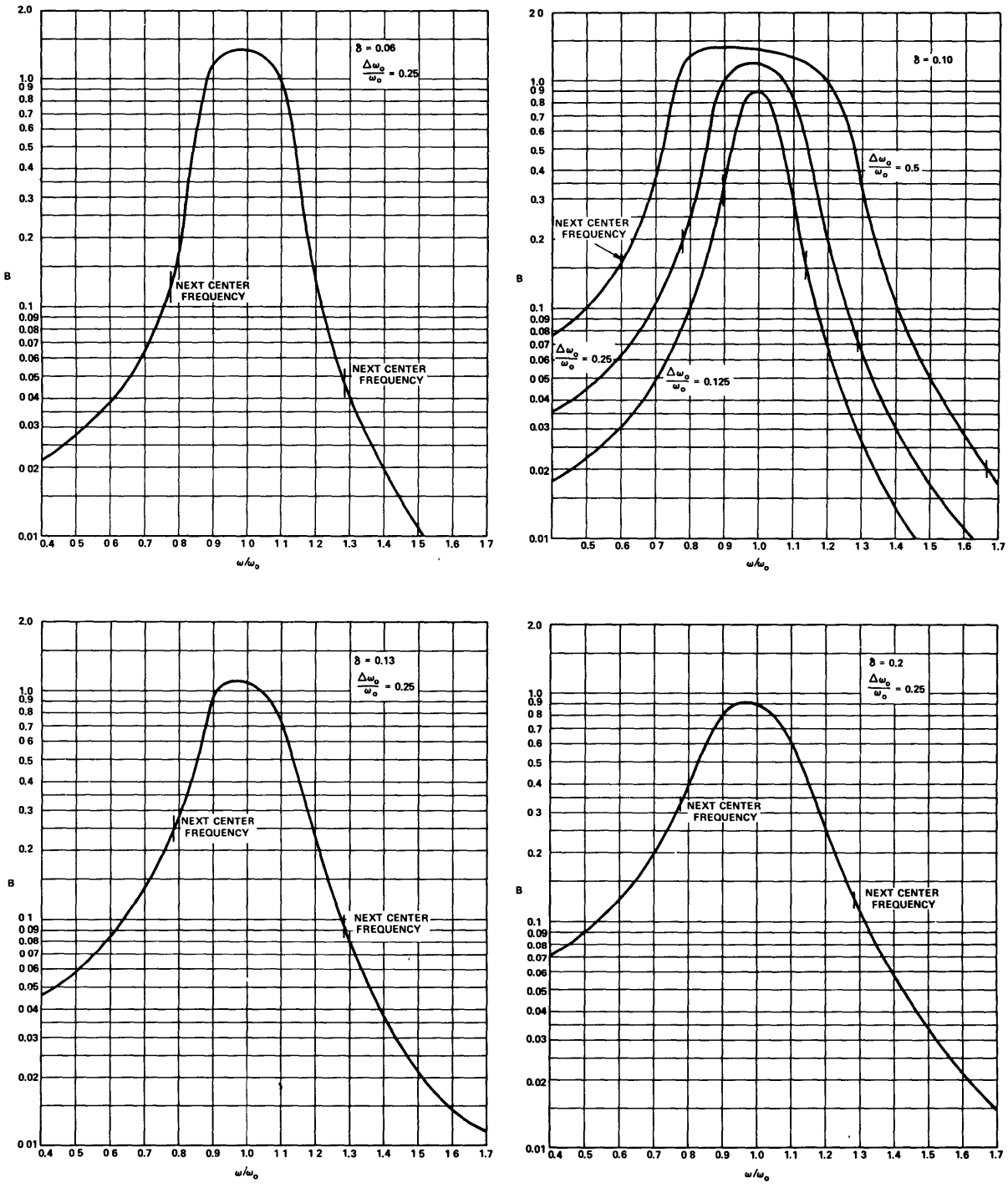

Figure 4 - Imaginary Component of Compressibility for Various Damping Constants and Bandwidths

$$\sim \frac{2\,\varepsilon_n}{\frac{\eta_n}{\gamma}\left[1 - \frac{2\sigma\left(1 - \frac{1}{3\eta_n}\right)}{R_{o_n}\left(P_o - P_v\right)}\right]} \qquad [45]$$

and if the denominator is put equal to unity (at low static pressures with $\nu \sim 10^5$, the denominator would vary between 0.8 and 1.2 in a typical frequency range whereas it would be close to unity at high static pressures); then

$$a(\omega) = \frac{1}{\rho C_o^{\,2}} + \frac{\omega}{2\pi\left(P_o - P_v\right)\gamma}\sum_{n=1}^{N}\tau_n\left(2\varepsilon_n\right)$$

But $\varepsilon_n = \frac{\Delta\omega_{o_n}}{2\omega}$

$$\therefore \quad a(\omega) = \frac{1}{\rho C_o^{\,2}} + \frac{1}{\left(P_o - P_v\right)\gamma}\sum_{1}^{N}\frac{\tau_n\,\Delta\omega_{o_n}}{2\pi}$$

$$= \frac{1}{\rho C_o^{\,2}} + \frac{\nu}{\left(P_o - P_v\right)\gamma} \qquad [46]$$

where ν is the total concentration from Equation [37]. From Equation [30] the velocity is

$$c = \sqrt{\frac{1}{\frac{1}{C_o^{\,2}} + \frac{\rho\nu}{\left(P_o - P_v\right)\gamma}}} \qquad [47]$$

so that if the velocity at a low frequency were measured, the total free air content would be

$$\nu = \gamma\frac{P_o - P_v}{\rho}\left(\frac{1}{C^2} - \frac{1}{C_o^{\,2}}\right) \qquad [48]$$

Unfortunately, the experimental investigations to date have been limited at low frequencies by reflections of nearby structures while still measuring significant attenuation, and thus it has not been possible to obtain a sufficiently low frequency to perform this valuable check of the computed total concentration of free air. Two investigations[21,22] have been formulated on the basis of Equation [48], neither has yet been used as a check of the total concentration as determined from the spectrum measurements.

As the equations are now formulated, with a known bubble distribution which would either be in the form of a step function or approximated as such, the attenuation and velocity at a given frequency ω could be calculated as follows. The width of each step in the bubble distribution would be expressed as a frequency increment using Equation [14] to give the resonant frequency corresponding to the radius. Then for midinterval values, the damping constant and the polytropic expansion coefficient could be calculated from the equations in Appendix A. Next, Equations [43] and [44] would be evaluated and, finally, Equations [28] and [29] would give the velocity and attenuation. This procedure could be followed for a number of frequencies to obtain the velocity and attenuation as a function of frequency. Then the propagation of the wave could be calculated by resolving an arbitrary wave into its Fourier components.

To check the calculation procedure, the bubble distribution determined photographically by Fox, Curley, and Larson[8] was used to calculate the velocity and attenuation. The amount of free air in these tests is much greater than found by Ripkin and Killen[12] in a water tunnel, but it might be representative of either very low pressures in a tunnel or of wakes of high-speed surface ships. These data are particularly interesting since both phase velocity and attenuation were measured over a range of frequencies. Unfortunately, their results are presented in small graphs and the bubble distribution is averaged whereas the measured attenuation and phase velocities are not. The authors state that repeat evaluations for the bubble distribution did not vary radically. All of the data are shown in Figure 5. Independent of the bubble distribution evaluation, the free-air content was measured and found to be $2.0 \pm 0.5 \cdot 10^{-4}$ by volume. Their bubble distribution curve was scaled to give the median air content and

calculations made for attenuation and phase velocity. Comparisons are made with the experiments in Figure 5 for the median air content. Two different sets of calculations are given, one with the computed damping coefficient and one with a constant damping coefficient of 0.2 (maximum calculated damping coefficient is 0.14 for these data). The comparison indicates that the data fit best with the damping held constant at 0.2. However, direct measurements of the damping[14,15,23] do not generally give such a high value. (Maximum observed damping constant is 0.2 for air bubbles in water.[14,15]) Some of the physics not taken into account analytically (e.g., surface oscillations and off-resonant damping) might explain the less accurate predictions with computed damping but as noted in the Discussion section, these effects are not expected to be significant.

Both of the calculations are considered to be in good agreement with the measured data. The $\delta = 0.2$ calculations follow the apparent trends in data slightly better than the curve for computed damping. These calculations were made for the median air content. If the average had been slightly lower, the agreement with experimental data would have been even better. If the bubble distribution curve were a multiple of that given, the maximum attenuation would be proportional to concentration. For the minimum air content, the maximum attenuation would be 28 db/cm for the computed damping case and 25 db/cm for the constant damping case. For the maximum air content, the maximum attenuation would be 47 db/cm for the calculated damping and 42 db/cm for constant damping coefficient. A calculated curve somewhere between the median and low air content curves would be in excellent agreement with the measured attenuation. A lower total air content would also help the agreement with measured velocities.

BUBBLE SPECTRUM COMPUTATIONS

Calculations performed in the previous section explicitly found the attenuation and velocity at a given frequency ω when the bubble distribution is known. However, the problem is to determine the bubble distribution from measurements that can be performed on the water used in the test. The measurements of attenuation and velocity as a function of frequency are easily made. For the small concentrations expected in the majority of tests, the velocity will be near that of the bubble-free water

BUBBLE RADIUS m. m.	FREQUENCY CHANGE ACROSS BAND KHz	CENTER FREQUENCY KHz	$\frac{\Delta\omega_o}{\omega_o}$	BAND CONCEN-TRATION x 10^4	τ x 10^9	δ	$\left[1+\frac{2\sigma(1-\frac{1}{3\gamma})}{(P_o-P_v)R_o}\right]\cdot\frac{\eta}{\gamma}$
.011							
	134	204.00	.658	.0059	.0044	.1398	.856
.022							
	44 9	114.55	392	.0875	.197	.1252	.878
.033							
	22.7	80 75	.281	.1767	777	.1137	890
.044							
	13.6	62 60	.217	.331	2.437	1052	.9
.055							
	9.1	51 25	.1777	.454	4,990	.0990	.904
.066							
	6.5	43.45	.1496	.3425	5 270	0937	.911
.077							
	5.0	37 70	1326	.3605	7.210	.0893	918
.088							
	3.9	33.25	.1173	1222	3.135	0860	.922
.099							
	3.05	29 775	.1024	.0795	2.605	.0828	.928
.110							
	2.5	27 00	0926	.0392	1.569	.0799	.930
.121							

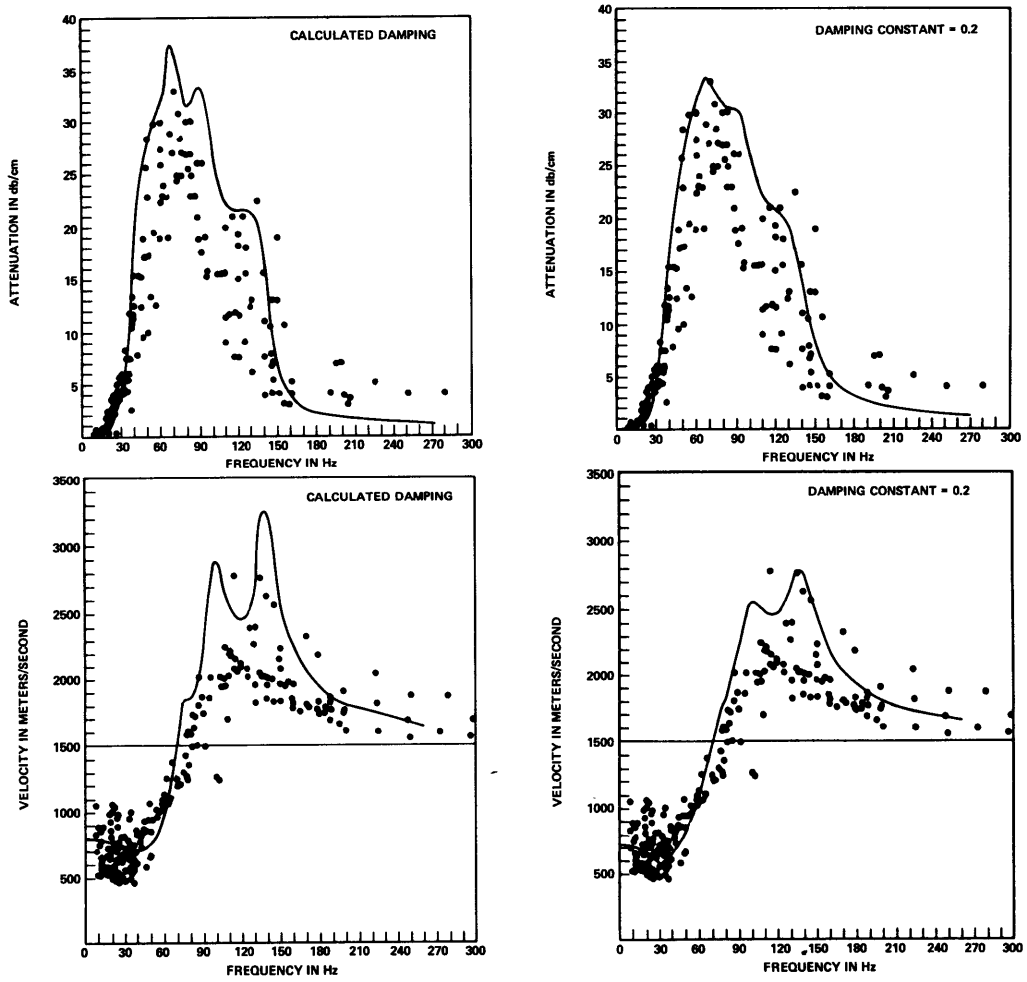

Figure 5 - Comparison of Computed and Measured Velocity and Attenuation

whereas the attenuation will be much greater than that for bubble-free water and hence less sensitive measuring instruments could be used than for the velocity and still retain the same accuracy in the resolved data.

With an iteration process, the equations of the previous section can be directly used to find the concentrations of the bubbles in the various bands. Thus for the m band, m being any of the n, the concentration function would be

$$\tau_m = \frac{\dfrac{\alpha(\omega)\, 4\pi\gamma\left(P_o - P_v\right)}{\rho\, \omega^2\left[C_o + \Delta c(\omega)\right]} - \sum_{n \neq m} \tau_n\, B_n}{B_m} \qquad [49]$$

where the notation on the summation sign means that the m^{th} term is omitted. The band volume concentration would be $\tau_m \Delta \omega_{o_m} / 2\pi$* from Equation [36].

This expression would hold for any of the m and any ω. If the m^{th} band whose center frequency ω_m corresponds to the driving frequency ω is chosen, then the summation term will be only a small fraction of the measured attenuation and thus a good iteration scheme is set up.

COMPUTER PROGRAM

To quickly and accurately determine the bubble distribution from the measured attenuation, a computer program was written in FORTRAN IV language. Program compilation and complete data analysis on the IBM 7090 takes less than a minute, and each additional data set is analyzed in only a few seconds more.

---

*This is the total volume of gas per unit volume of gas-liquid mixture in the band of radii with endpoints separated by $\Delta \omega_{o_m}$. It does not mean that each radius in the interval has this concentration.

The data needed to calculate the bubble distribution from attenuation measurements are the frequency and attenuation per unit length over a suitable range of frequencies and the test conditions of pressure, distance between hydrophones, specific heat at constant pressure for the gas, thermal conductivity for the gas, coefficient of viscosity of the liquid, density of the liquid, speed of sound in bubble-free liquid, adiabatic expansion constant for the gas, surface tension for the liquid-gas interface, vapor pressure of the liquid, and a number relating pressure and density of the gas.* Provision is made in the program for input of attenuation either as decibels with the known path length or as voltage levels seen on the receiving hydrophone and the distance between hydrophones. Internal to the program, physical constants are provided for a temperature of 26.7 C (80 F) for air bubbles in water.

The calculation procedure used in the program is that just presented. The input data from either option are first converted to common units of nepers per centimeter, then each two consecutive points are averaged for midband values, and the bandwidth is obtained by subtracting each frequency from the one following it. The damping and polytropic expansion coefficient (see Appendix A for equations) are next calculated using Devin's expressions.[18] The propagation matricies A_n and B_n (defined in Equations 43 and 44) are then calculated. To get the iteration started, the concentration function τ is found by taking m a value near the halfway point of the input data and solving Equation [49], ignoring both the summation and the increment in velocity. This same value is given to all the τ as a first guess. With this first guess concentration, the velocity can be calculated at the highest frequency and the summation in Equation [49] for m = N performed. Then τ_N is found from Equation [49]. This new value of τ_N then replaces the first estimated value and the process is repeated for τ_{N-1}. These steps are repeated for all the m from highest to lowest center frequency. At each point, the ratio of old to new value of τ is determined for use as the convergence criteria. The whole process just outlined is repeated until the present and previous values of τ at each and every point agree to within at least 0.1 percent.

---

*The effects of the physical constants on the computed results for air bubbles in water are discussed in the following section.

FORMAT FOR DATA INPUT

Each set of data to be converted to bubble concentrations consists of the following groups of cards: a control card, a title card, a card listing the static pressure and distance between hydrophones, cards for the experimental data, and then the option cards. Whether or not a group of option cards is used depends on the control card. Either or both of the option cards may be required. They are read in the following order: physical constants which would give different parameters than those at 26.7 C (80 F) given internally, and/or initial guesses for the bubble concentration function at each midband.

In order of use, specific instructions for the input cards are as follows:

Card 1, control card, Format 5I2

Column	Variable Identification and Comments
1- 2	JOBS, an integer if more data follow, zero if last set given.
3- 4	NOF, integer number of data points.
5- 6	IP, an integer if attenuation is given in decibels, zero if pressures are given with and without bubbles.
7- 8	ICON, an integer if the program values of physical parameters are used, zero if values are given.
9-10	ITAO, an integer if values for the first trial guess of concentration function is given, zero otherwise.

Card 2, identification card, Format 12A6

Column	Identification and Comments
1-72	TITLE, ZA, ZB, ZC, ZD, ZE, ZF, ZG, ZH, ZI, ZJ, ZK, any printable statement.

Card 3, pressure and distance card, Format 2F12.6

Column	Identification and Comments
1-12	PO, static pressure in atmospheres at depth attenuation is measured.
13-24	DIST, distance in centimeters between sending and receiving hydrophones.

Card 4, measured attenuation, as many cards as data points

(A) Option 1, If IP = 0, pressures are given from low to high frequency, Format 3F12.6

Column	Identification and Comments
1-12	FO(I), frequency in Hertz.
13-24	PWO(I), pressure received without bubbles in water.
25-36	PW(I), pressure received under test conditions.

(B) Option 2, If IP is an integer, attenuation in decibels is given from low to high frequency, Format 2F12.6.

Column	Identification and Comments
1-12	FO(I), frequency in Hertz.
13-24	ATN(I) Attenuation in decibels.

Cards 5, option cards for physical constants, used only if ICON is zero, Two cards, first card Format 6F12.6, second card Format 3F12.6.

Column	Identification and Comments
1-12	SP1, specific heat at constant pressure for air.
13-24	XK1, thermal conductivity for air in calorie/cm sec deg C.
25-36	YMU, coefficient of viscosity for water in poise
37-48	RHO2, density of water in grams/ml.
49-60	CO, speed of sound in bubble-free water in cm/sec.
61-72	XGAMA, ratio of specific heats for air.
1-12	SIGMA, surface tension for water-air interface in dynes/cm.
13-24	PV, vapor pressure of water in dynes/cm^2 (1 atmosphere = $1.013 \cdot 10^6$ dynes/cm^2).
25-36	CON3, factor to multiply static pressure (P_o) to obtain density of air in gm/ml at prevailing temperature.

Cards 6, Option cards for initial trial concentration guess, used only if ITAO is an integer. One less than the number of input data are needed, Format 6F12.6

Column	Identification and Comments
1-12	TAO(1), initial guess for τ of bandwidth at lowest frequency.
13-24	TAO(2), initial guess for τ of second frequency interval continued as needed.

CODING FORM FOR IBM TYPE 704 COMPUTER
NDW TMB 10462/9(719)

TITLE _____ PROGRAMMER _____ DATE _____

PROBLEM NO. _____ PHASE _____ LABEL _____ SHEET _____ OF _____

SYMBOL	OP.	ADDRESS, TAG, DECREMENT	REMARKS	IDENT	NO.
6		18 30 42 54 66			
010400010 1					
		INIT TAØ=0.	COMPUTER TRIAL DATA 4 PØINTS 5/68		
.5		16.0			
10000.		1.2	1.0		
30000.		2.2	1.0		
50000.		2.65	1.0		
100000.		1.17	1.0		
001100010 0					
			COMPUTER TRIAL DATA II PØINTS 5/68		
.5		16.			
10000.		1.2	1.0		
12590.		1.33	1.0		
15830.		1.47	1.0		
19930.		1.69	1.0		
25100.		1.96	1.0		
31580.		2.26	1.0		
39750.		2.5	1.0		
50000.		2.65	1.0		
62900.		2.65	1.0		
79200.		2.21	1.0		
100000.		1.17	1.0		

Figure 6 - Typical Data Input to Computer Program

Typical input data are shown in Figure 6. Initial guesses of zero for the concentration function were made in the first case and the internal physical constants are used. The second case is a repeat of the first with no initial estimates and more data points.

TYPICAL OUTPUT

As will be discussed in the next section, an arbitrary curve was selected to represent the test data. The analysis of these data are shown in Figure 7.

The top of the first page of output gives computed results for the radius of bubble resonant at the input frequency and for the damping constant. Information on the columns is as follows: the frequency is in Hertz, the two amplitudes are relative to each other (the ratio is used to determine the attenuation in decibels, and this is divided by the distance between measuring points to obtain the attenuation per unit length), the bubble radius is given in centimeters, and the damping is nondimensional.

The bottom half of the page gives the band values which are averages of the input data. The frequencies are again given in Hertz. The first column is the center frequency, the second and third columns the end frequencies of the band in Hertz, the fourth column is the change in frequency across the band in Hertz, and the last column is the average attenuation in the band converted to nepers per centimeter.

A series of pages following the averaged values will give the results of each step in the iteration to find τ, the concentration function. For illustration, the first page is shown. As can be seen, the higher frequencies are first evaluated. The first column is again the center frequency in Hertz. The second column is the velocity ratio, the computed velocity divided by the bubble-free velocity. The third and fourth columns are values for the concentration function. The third column is the previous concentration and the fourth column is the new value. The last column is the ratio of the two τ's. Assuming τ a constant was not a good guess here. The value of the concentration function determined in the first line is used in the computations for other values. Once the second concentration is determined, it is also used in determining subsequent values.

BUBBLE SPECTRUM ANALYSIS

TEST DATA

11 PTS COMPUTER TRIAL DATA 5/68

P(STATIC)=0.5000 ATMOS.16.000 CM BETWEEN PROBES

FREQUENCY	AMPL W/O	AMPL W/	ATTN DB/CM	R,CM	DAMP
10000.0	1.200000	1.000000	0.098977	0.021233	0.088707
12590.0	1.330000	1.000000	0.154815	0.016776	0.095501
15830.0	1.470000	1.000000	0.209147	0.013268	0.102357
19930.0	1.690000	1.000000	0.284858	0.010475	0.109276
25100.0	1.960000	1.000000	0.365320	0.008263	0.116049
31580.0	2.260000	1.000000	0.442636	0.006522	0.122043
39750.0	2.500000	1.000000	0.497425	0.005143	0.126057
50000.0	2.650000	1.000000	0.529057	0.004060	0.126553
62900.0	2.650000	1.000000	0.529057	0.003210	0.122738
79200.0	2.210000	1.000000	0.430490	0.002543	0.115220
100000.0	1.170000	1.000000	0.085232	0.002017	0.105651

FREQUENCY PARAMETERS

F0	F1	F2	DELTA F	ATTN NP/CM
11295.0	10000.0	12590.0	2590.0	0.014609
14210.0	12590.0	15830.0	3240.0	0.020951
17880.0	15830.0	19930.0	4100.0	0.028437
22515.0	19930.0	25100.0	5170.0	0.037427
28340.0	25100.0	31580.0	6480.0	0.046510
35665.0	31580.0	39750.0	8170.0	0.054114
44875.0	39750.0	50000.0	10250.0	0.059089
56450.0	50000.0	62900.0	12900.0	0.060910
71050.0	62900.0	79200.0	16300.0	0.055236
89600.0	79200.0	100000.0	20800.0	0.029687

A. FIRST PAGE OF OUTPUT

ITERATION NO. 1

FREQUENCY	VR(I-1)	TAO(I-1)	TAO(I)	RATIO
89600.0	1.025584	0.316E-10	0.491E-12	64.4083C6
71050.0	0.982403	0.316E-10	0.808E-11	3.912918
56450.0	0.964866	0.316E-10	0.158E-10	1.997114
44875.0	0.955481	0.316E-10	0.256E-10	1.234318
35665.0	0.949876	0.316E-10	0.380E-10	0.830822
28340.0	0.946341	0.316E-10	0.519E-10	0.608447
22515.0	0.944037	0.316E-10	0.657E-10	0.481336
17880.0	0.942438	0.316E-10	0.783E-10	0.403880
14210.0	0.941072	0.316E-10	0.908E-10	0.347918
11295.0	0.939026	0.316E-10	0.101E-09	0.314317

B. SECOND PAGE OF OUTPUT

COMPUTED BUBBLE SPECTRUM

11 PTS COMPUTER TRIAL DATA 5/68

P(STATIC)=0.5000 ATMOS.16.000 CM BETWEEN PROBES

FREQUENCY	VELOCITY	TAO	CONCENTRATION	R,CM	DAMP	NO BUB/CC	A	B
11295.0	0.942618	0.102E-09	0.263E-06	0.018747	0.092281	0.954E-02	0.500E-10	0.292E-11
14210.0	0.954362	0.862E-10	0.279E-06	0.014820	0.099117	0.205E-01	0.487E-10	0.328E-11
17880.0	0.963096	0.731E-10	0.300E-06	0.011710	0.106019	0.446E-01	0.478E-10	0.351E-11
22515.0	0.972159	0.606E-10	0.314E-06	0.009241	0.112901	0.949E-01	0.469E-10	0.363E-11
28340.0	0.981770	0.474E-10	0.307E-06	0.007292	0.119375	0.189E 00	0.460E-10	0.355E-11
35665.0	0.990985	0.346E-10	0.282E-06	0.005752	0.124514	0.354E 00	0.452E-10	0.325E-11
44875.0	0.998945	0.235E-10	0.241E-06	0.004538	0.126837	0.616E 00	0.445E-10	0.280E-11
56450.0	1.005573	0.153E-10	0.197E-06	0.003585	0.125068	0.102E 01	0.439E-10	0.228E-11
71050.0	1.011107	0.884E-11	0.144E-06	0.002837	0.119126	0.151E 01	0.434E-10	0.163E-11
89600.0	1.012151	0.263E-11	0.547E-07	0.002248	0.110271	0.115E 01	0.434E-10	0.696E-12

TOTAL CONCENTRATION= 0.238E-05

PHYSICAL CONSTANTS

SPI	K	MU	RHO	C	GAMMA	SIGMA	PV	CON3
0.240000	0.000062	0.008603	0.996540	150300.00	1.400000	71.420000	35050.00	0.001178

C. LAST PAGE OF OUTPUT

Figure 7 - Typical Data Output from Computer Program

The particular set of data shown here took six iterations to complete. The solution is shown on the last page of data output. The first column is again the center frequency in Hertz. The second column is the velocity ratio and the third column is the concentration function τ. The fourth column is the concentration which is the product of the concentration function and the change in frequency across the band from page 2 of the output. The radius and damping are given next for the center frequency. The number of bubbles per cubic centimeter is next determined by assuming they are all of the same size as the center band radius. The concentration is divided by the volume of a single bubble to get the bubble density. The last two columns are the a and -b in Equations [43] and [44].

Underneath the band data is printed the summation of the concentrations to give the total free gas. Below this are printed the physical constants which were used in the analysis--the values are in cgs (centimeter-gram-second) units as required in the input format.

INVESTIGATION OF METHOD

As is generally the case, the mathematical analysis does not directly provide guidance for data collection. In order to evaluate the effects of number of points, point distributions, different physical constants, and typical errors, computer computations were made using an assumed data curve. The arbitrary curve used to represent the ratio of pressures received with and without bubbles is shown in Figure 8. For all tests, air and water were the two phases and variables were assumed pertinent to water-tunnel operations.

The first check was to determine the number and spacing of data points needed to determine an accurate estimate of the total free gas. In all studies, the first data point was at 10.0 kHz and last point was at 100.0 kHz. First a fine grid of points at an arbitrary spacing was taken. Points were progressively reduced while both the concentration function and total concentration were recorded. The location of the points in the interval was also varied during the study. The calculations showed that 10 intervals of equal percent bandwidth were sufficient to give accuracy in the total concentration within 1/2 percent of that at 30 points (asymptotic

value). Also the spacing that produced the best accuracy was found to be constant percentage bandwidth. For the 10 intervals just mentioned, the ratio from one measuring frequency to the next was about 1.259. Accuracy to within 10 percent was possible with only five points in the interval 10 to 100 kHz. Here too the accuracy was increased by using constant percentage bandwidth analysis (i.e., more points at lower frequencies) rather than selecting the point spacing so that averaged attenuation values would fall nearer the curve in Figure 8. Individual band concentrations were off more than the total concentration, with most of the differences occurring at the higher frequencies (smaller bubble sizes) although when only three bands were used (total concentration about 15 percent low), the end bands were both low. Undoubtedly much of this was because the averaged attenuation was not near the curve value, but no checks were made since the determination of points experimentally is considered more of a problem than running the computer program. In other words, if more points were available from the experiments, they would have been used.

In view of the improved prediction of the measurements in Reference 8 when the damping constant was taken as a constant 0.2, the effect of damping on the computed bubble spectrum was investigated. For the sample computer run (Figure 7), the damping constant was changed to 0.2 and the results reanalyzed. A comparison is shown in Figure 9. In the first case with computed damping, the effect of each band is confined to a region near resonance and a smooth variation is obtained in the bubble distribution. With the large damping, the band effect is spread out and the end points in the bubble spectrum do not fit into the curve as well. It is interesting that an approximate 200-percent increase in damping causes only a 5-percent increase in free gas, indicating that the damping is not critical. With this high damping constant, other assumed data curves which were less smooth would occasionally have zero for intermediate band concentrations. (The computer program sets any negative concentrations to zero.) With the large damping constant, more iterations were required for convergence.

Checks were then made for the effects of the physical properties on the computed concentration. The effect will be considered on total free air content which generally influences the bubble spectrum more at the higher frequencies (small bubbles) than at the lower frequencies. A

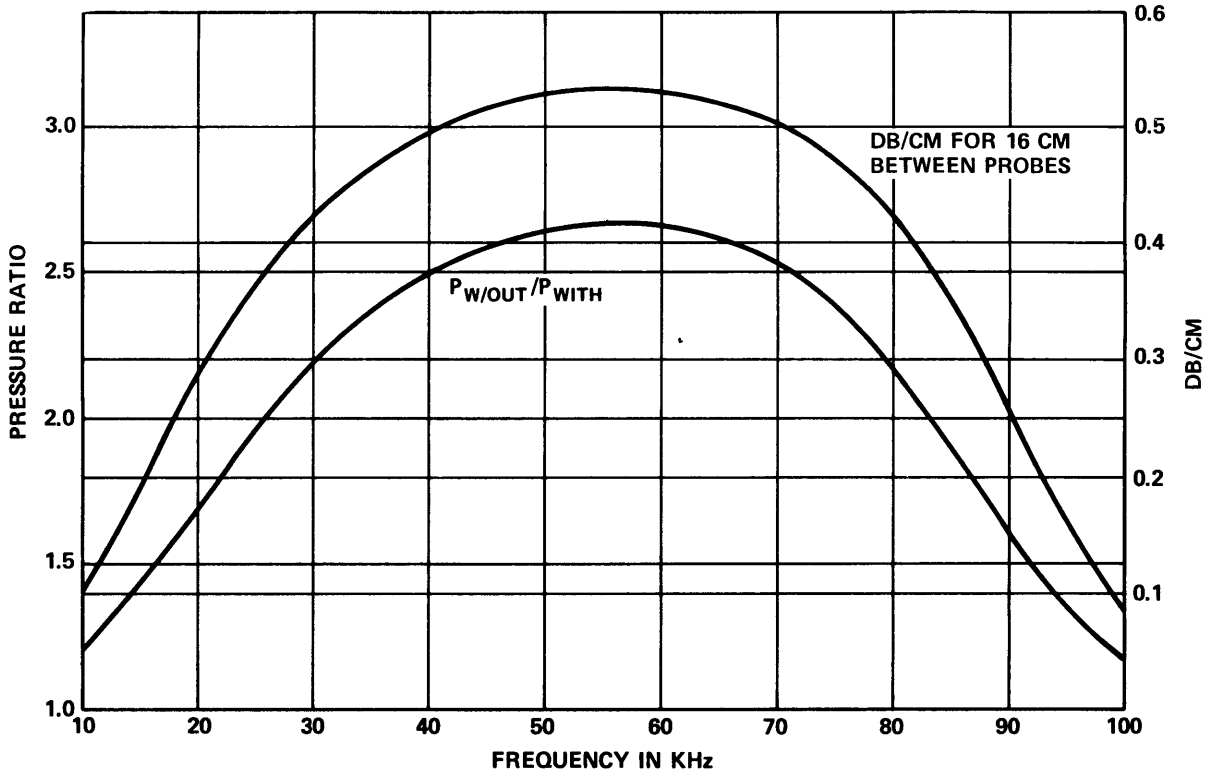

Figure 8 - Assumed Data Curve for Computer Trial Analysis

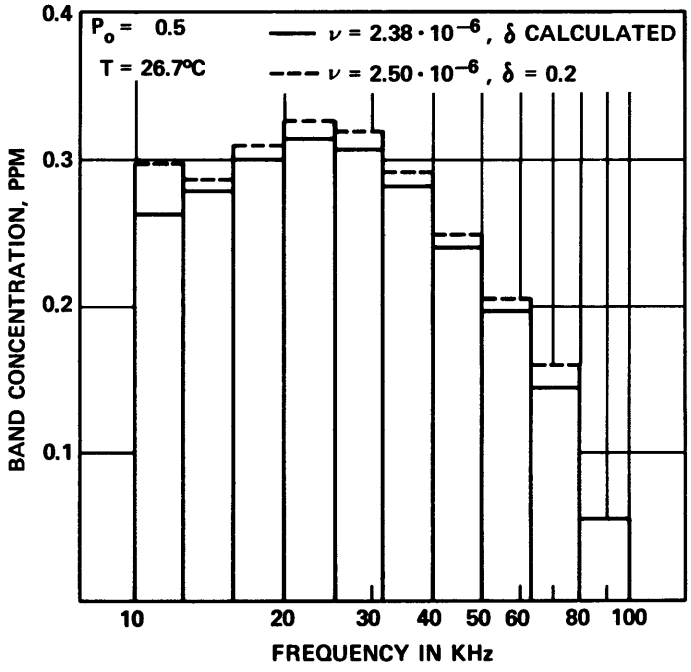

Figure 9 - Comparison of Bubble Distributions Calculated with Computed Damping and with Constant Damping 0.2

50-percent reduction in surface tension reduced the free air concentration 9 percent at a static pressure of 0.2 atmospheres and less than 1 percent at atmospheric pressure. A 50-percent increase in viscosity increased the free air by about 1 percent at 0.1 atmosphere pressure and negligibly at atmospheric pressure. A 15-percent increase in the thermal conductivity reduced the concentration by about 1 percent at half an atmospheric static pressure and about 1/2 percent at 0.1 atmosphere and 1 atmosphere. A 10-percent increase in the constant relating air pressure to density gives about 1-percent increase in the free air. A 1-percent change in water density produced a 1-percent change in concentration; a 1-percent change in the speed of sound in bubble-free water also gave a 1-percent change in concentration and so did a similar change in pressure. The water density, speed of sound, and pressure are multiples of the dominant term on the right-hand side of Equation [49]. Since the specific heat at constant pressure for air and the ratio of specific heats do not change for the expected range of temperatures or pressures, they were not investigated. The various changes just mentioned in the constants had little effect on the speed of sound as calculated from the computed bubble distribution.

The effect of temperature changes was also examined for identical measurements. At half an atmosphere static pressure, a change in physical constants caused by a temperature rise from 15.6 C (60 F) to 20 C (68 F) decreased the computed free air by 3 percent. A rise from 20 to 26.7 C (80 F) resulted in a 4-percent decrease in the free air. In these calculations, the effect was more uniformly distributed over the spectrum than with changes in individual constants. At 0.1 atmosphere pressure, the changes were 6 percent for the 15.6 to 20 C change and 12 percent for the 20 to 26.7 C change, and at 1.0 atmosphere, the changes were 2 and 3 percent, respectively.

Calculations were next made to determine the effects of the calculated polytropic expansion coefficient. The trial data shown in Figure 8 were analyzed for isothermal and adiabatic conditions. The isothermal analysis gave lower total free air contents than the polytropic and the adiabatic gave higher. The isothermal and adiabatic differed uniformally by approximately the gas constant γ (i.e., the adiabatic was 40 percent higher than the isothermal). At a static pressure of 0.1 atmospheres,

there were negligible differences in the polytropic and isothermal analysis. At 1 atmosphere static pressure, the polytropic was about 28 percent higher than the isothermal and about 9 percent lower than the adiabatic case. In both the adiabatic and isothermal analysis, concentration was directly proportional to pressure. The damping used in this study was that corresponding to the calculated bubble radius.

During the study of data point spacing, there were considerable differences in the shape of the bubble distribution curves with the different spacing, even though τ was consistent. For consistency in data, either τ must be considered the variable of interest or a uniform spacing must be used for the input data. Reporting actual concentrations (not τ) at constant percentage bandwidths is recommended.

The calculations were made for bubbles with resonant frequencies from 10 to 100 kHz. Bubbles with a different range of resonant frequencies and concentrations would be affected differently. For example, more pronounced changes could occur for distributions at higher frequencies.

DISCUSSION

The calculation method in this report differs from that prepared at Saint Anthony Falls Hydraulic Laboratory (SAFHL) mainly in details; some factors in their expressions could not be duplicated* and thus there is some difference in the final equations. The damping constant used in the SAFHL analysis is taken from experimental results for atmospheric pressure, whereas here it is calculated as a function of pressure (see Appendix A). Also SAFHL has found that linearizing the expressions involved in the acoustic propagation was adequate for their purposes. In the present study comparisons made with the linearized and nonlinear expressions for a typical case indicated that the total free-air content was about 6 percent greater

---

*Equation [12a] in Reference 12 should have a 2 in the denominator instead of $\sqrt{2}$. Their Equation [16a] has an extra factor of $(\omega/\omega_o)^2$ in the last term of the denominator. Notice also the differences between Figure 4 of this report and Figure 2A of Reference 12.

when the linearized expressions were used. The location of the spectrum peak was not changed (constant percent bandwidth analysis). However the peak location on the first iteration for each of the analyses was shifted two bands toward the higher frequencies and the total free air was about 5 percent higher than for the iterated solutions. Comparisons were not made directly with the SAFHL computed bubble distributions since the information given in Reference 12 was not sufficient to recompute their bubble distribution.

The method of analysis presented here is subject to question on two points: either the physics of the situation is not correctly taken into account or the analysis is not properly done.

Consider the analysis first. This is based on the equation of motion of a spherical bubble undergoing small motions. Damping proportioned to bubble wall velocity is introduced in the equation of motion. The equations are linearized for the small motions expected in acoustic excitation. The ordinary, linear second-order equation is solved for the change in radius due to a sinusoidally varying pressure. The compressibility is evaluated next and the propagation properties determined. An iteration procedure is used to work back from the propagation to the bubble distribution. As long as the driving pressure is kept low (see Appendix C), the analysis should be satisfactory. During the data collection, it was assumed that the phase velocity was near that of bubble-free water which would be true for low free-air contents. With larger free-air contents, the same assumption can be used since the phase velocity passes through the pure water value near the peak of the attenuation values. Thus larger free-air contents might be distorted somewhat but the peak should not be changed in the calculated bubble distribution.

Several possibilities for errors exist in the assumed physics of the problem: the calculated damping constant, possible surface oscillations, and possible nonuniformity of the liquid-bubble mixture.

For air bubbles in water at atmospheric pressure, the calculated damping constant at resonance appears to be confirmed by the theory although there is considerable scatter. Devin[18] ignores the scatter and concludes close agreement between theory and experiment for resonant damping at atmospheric pressure. Tests with water have been performed just to the point

where viscous effects start to be important (300 kHz) so no firm conclusions can be drawn about viscosity. However tests[23] in a more viscous liquid do not confirm the importance of viscous damping although not enough information is given to check the calculations. At the low static pressures employed in water tunnels, viscous damping is important in the working frequency range (see Appendix A).

Another problem with the damping is the off-resonance effects for which no experiments exist. Although Devin[18] and Hsieh and Plesset[17] give equations for which damping could be found as a function of frequency, there is not yet sufficient justification for including this in the development. For example, at atmospheric pressure, the damping is[18*]

$$\delta = 4.4 \cdot 10^{-4} \frac{f_o}{\sqrt{f}} + 1.4 \cdot 10^{-2} \left(\frac{f}{f_o}\right)^2 , \quad f_o < 10 \text{ kHz}$$

which at 10 kHz gives a damping constant at resonance of about 0.058. For a bandwidth of 25 percent, the center frequency of the closest neighboring band would be $7/9 \cdot 10$ kHz = 7.8 kHz. The damping at this off-resonance point is also approximately 0.058. Thus there is no effect on the neighboring point for this case. Assuming a similar frequency dependence for the damping constant at higher resonant frequencies gives a 5-percent change in the contribution to the neighboring interval for f_o = 50 kHz and the same 25-percent bandwidth. Since 20 percent of the band value at 50 kHz is added to the band at 38.8 kHz, the overall effect is only 1 percent of the 50-kHz value. Points further away are even less affected.

Investigations of damping have generally been made for a bubble in still water. Victor[24] has recently investigated the effects of directional motion on damping and found negligible influence for air bubbles in water.

Another physical effect which is not accounted for in the analysis is the possibility of nonspherical oscillations. Absorption would occur at

---

*The first term is due to thermal effects and the second to radiation. The radiation term differs from that quoted in References 8 and 13 by a factor of f/f_o.

resonant frequencies other than that given in Equation [14]. Strasberg[25] suggests that some anomalies in measured damping constants[23] could result from excitation of surface oscillations. The analysis presented here does not account in any way for surface harmonics, and it would appear to be a difficult problem to include these effects unless the amplitude of the various modes could be determined. Strasberg[26] has shown that the resonant frequency of volume pulsations for oblate spheriods is only slightly different from that of spheres. In calculating absorption of a bubble in general motion, Hsieh and Plesset[17] found that when the wavelength is much greater than the bubble radius, the damping is essentially due to volume pulsations and confirmed the resonant frequency to be that for volume pulsations. This indicates that surface oscillations are relatively unimportant. Meyer and Tamm[27] measured sound pressures and surface oscillations for air bubbles in water. Although not conclusive, absorption appears to occur only at the volume resonance in the data they present.

Nonuniformity in the flow could cause spurious reflections and make invalid the assumption of an homogeneous medium needed in Equation [18]. If bubbles were to be clumped together, for example, reflections might arise which would be caused by the acoustic impedance change due to the grouping.[15]

The necessary conditions on the bubble-liquid mixture so that properties can be considered uniform are not known precisely. The bubble size should be at least an order of magnitude less than the wavelength of sound. The cumulative effect of the bubbles is assumed additive and thus they must be far enough apart so that there are no interactions. Spitzer has examined the spacing of bubbles and concludes that a spacing of 5 R_o is sufficient for negligible interactions. For a radius of 0.1 mm, this is a bubble density of 8×10^3 per cubic centimeter, or a free-air content independent of radius, of 0.03 by volume. This is an excessive amount of air. The minimum number of bubbles that should be present is more a function of convenience than a mathematical limit. As shown in the test results, with a small free-air content (Appendix C), there is considerable variation in the received signal. It is postulated that these variations are due to the small volume of water sampled by the receiver, that is, only occasionally do bubbles of the correct size to produce attenuation flow into the measuring

volume. Unfortunately, the variations in received signal increase with frequency and, for these data, the number of bubbles per unit volume also increases with resonant frequency. This point is thus unresolved and more work should be done on the minimum number of bubbles needed in the mixture.

Other minor effects are ignored. For example, the density of the bubble contents is computed for air at the specified static pressure. Actually the pressure inside the bubble is slightly greater than this due to surface tension while the presence of the water vapor lowers the overall density. The effect of changes in the bubble contents density have been shown to be small in the section termed Investigation of Method. Also the thermal conductivity is affected by the water vapor but its effects are also relatively small as pointed out in the preceding section. Since oxygen is more soluble in water than is nitrogen, the constants for the gas properties could also be affected by the different balance, but they are ignored. In addition, the surface tension is known to be affected by trace contaminents but its effect is also small. Thus the constants which are most in doubt affect the overall accuracy only in a minor way.

The best way to check the overall accuracy of the method would be an independent determination of the bubble distribution (e.g., photographically) together with the attenuation measurements. This is what has been done by Fox, Curley and Larson.[8] As previously explained, the computed results are considered in good agreement. The answers from this analysis were input into the program for bubble distribution analysis and the spectrum could be duplicated within about 1 percent.* Thus the analysis is consistent and the iteration scheme does not introduce any new problems.

SUMMARY AND CONCLUSIONS

A procedure is examined for evaluating a gas bubble distribution in a liquid medium from the measured attenuation. The analysis consists of the calculated response of a single spherical bubble to forced harmonic motion and summing the individual responses to obtain the cumulative

---

*Most of this is felt to be caused by cumulative errors in some of the hand work required.

acoustic effect. The total effect of the bubbles is assumed to produce a uniform medium with a complex compressibility which can be resolved into phase velocity and attenuation. An iteration procedure is used to resolve the bubble spectrum from the measured attenuation.

A computer program has been written which quickly evaluates the bubble distribution. Using this program, the calculations for air bubbles in water are shown to be fairly insensitive to those physical properties of the environment which are most in doubt. The items which have the largest effect on the calculations are attenuation, static pressure, water density, and speed of sound in bubble-free water. Accuracy in these variables directly affects the calculated distribution.

The method presented here for bubble analysis is intended for use with off-the-shelf items which should be available in most laboratories. Appendix C describes the instrumentation used at this Center and explains the procedure used in the water tunnel. The two most attractive features of the method are the low cost of instrumentation and the ease with which the equipment can be operated by inexperienced personnel.

The ability to duplicate measured attenuation and phase velocity from the analytical results is encouraging, but several points in the analysis need further verification. The most important of these is the damping constant. Its value off-resonance and as a function of static pressure should be experimentally investigated. The unknown effects of bubble shape and surface oscillations need to be investigated as does the minimum concentration of bubbles. In addition to this check of steps in the analysis, an independent determination of a bubble distribution is also needed to evaluate the overall method.

ACKNOWLEDGMENT

Discussions with Marlin L. Miller were very instructive during the experimental portion of this work.

APPENDIX A

BUBBLE DAMPING

The damping constant can be calculated from the equations in Reference 18. The damping can be divided into three components--thermal absorption, reradiation, and viscous dissipation. The equations for calculating each of these are:

Thermal Absorption

$$\delta_{TH} = \frac{\frac{\text{SINH X + SINX}}{\text{COSH X - COSX}} - \frac{2}{X}}{\frac{X}{3(\gamma-1)} + \frac{\text{SINH X - SIN X}}{\text{COSH X - COS X}}}$$

where

$$X = \sqrt{\frac{2\rho_1 \, Sp_1 \, \omega_o}{k}} \, R_o$$

ρ_1 is the density of air,

Sp_1 is the specific heat at constant pressure for air, and

k is the thermal conductivity of air.

Reradiation

$$\delta_{RAD} = \frac{1}{C_o}\sqrt{\frac{3\gamma\left(P_o - P_v\right)\eta}{\rho \quad \gamma}\left[1 + \frac{2\sigma}{R_o\,(P_o - P_v)}\left(1 - \frac{1}{3\eta}\right)\right]}$$

where

$$\frac{\gamma}{\eta} = \left(1 + \delta_{TH}^2\right)\left[1 + \frac{3(\gamma-1)}{X}\left(\frac{\text{SINH X - SIN X}}{\text{COSH X - COS X}}\right)\right]$$

Viscous Dissipation

$$\delta_{vis} = \frac{4\mu\omega_o}{3\gamma\left(P_o - P_v\right)\frac{\eta}{\gamma}\left[1 + \frac{2\sigma}{R_o\left(P_o - P_v\right)}\left(1 - \frac{1}{3\eta}\right)\right]}$$

where μ is the coefficient of viscosity.

And the total damping constant is the sum of the three components:

$$\delta = \delta_{TH} + \delta_{RAD} + \delta_{VIS}$$

Although it is not obvious from the way the equations are presented, an iteration must be used here to find the radius since the polytropic expansion coefficient also enters the equation for the radius; see Equation [14].

The damping constant is shown in Figure 10 as a function of static pressure and frequency. Although the components are not shown in the figure, the contribution of each is clear. The radiation component is nearly a constant, the thermal component accounts for the peak, and the viscous component causes the curve to increase at the high frequency end.

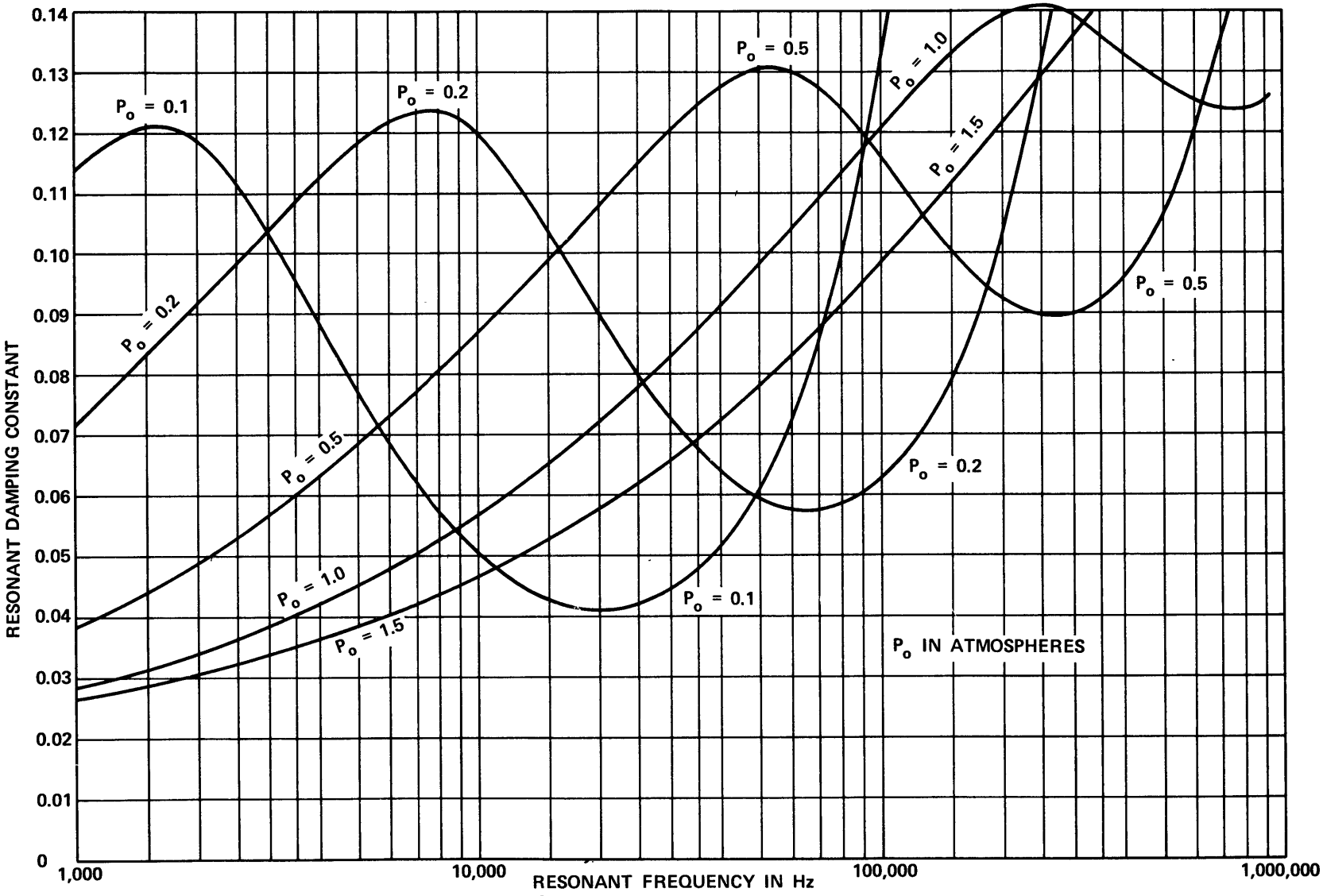

Figure 10 - Theoretical Damping Constant for Resonant Air Bubbles in Water

BLANK

APPENDIX B

LISTING OF STATEMENTS IN COMPUTER PROGRAM

```
C BUBBLE SPECTRUM ANALYSIS
C          T BRCCKETT,CODE 526 B, EXT 3136   APR 68
C
      DIMENSION FO(60),F1(50),F2(50),ATN(50),Z1(50,50),Z2(50,50),
     1   B1(50,50),A1(50,50),TAO(50),VR(50),RO1(50),XG(50),ETA(50),
     2       DELF(50),PWO(50),PW(50)
      COMMON FC,     PO,NOF,PI,RO1,XG,ETA,XGAMA,RHO2,CO,Z1,B1,A1,Z2
      COMMON     SP1,XK1,YMU,                SIGMA,PV,CON3
C
      PI=3.1415927
C
C READ CONTROL CARD AND TEST DATA
C
  100 READ(5,1) JOBS,NOF,IP,ICON,ITAO
      READ(5,12) TITLE ,ZA,ZB,ZC,ZD,ZE,ZF,ZG,ZH,ZI,ZJ,ZK
      READ(5,2) PO,DIST
      WRITE(6,3)
      WRITE(6,12) TITLE,ZA,ZB,ZC,ZD,ZE,ZF,ZG,ZH,ZI,ZJ,ZK
      WRITE(6,13)PO,DIST
      IF(IP) 107,104,107
  104 DO 105 I=1,NOF
      READ(5,2) FO(I),PWO(I),PW(I)
  105 ATN(I)=      ALOG(PWO(I)/PW(I))/DIST* 8.6858896
      GO TO 109
  107 DO 108 I=1,NOF
      READ(5,2) FO(I),ATN(I)
      PWO(I)=0.0
      PW(I)=0.0
  108 ATN(I)=ATN(I)/DIST
  109 IF(ICON) 300,301,300
  300 SP1=.24
      XK1=.0000623
      YMU=.008603
      RHO2= .99654
      CO=150300.
      XGAMA=1.4
      SIGMA=71.42
      PV=35050.
      CON3=.001178
      GO TO 302
  301 READ(5, 2) SP1,XK1,YMU,RHO2,CO,XGAMA,SIGMA,PV,CON3
  302 CALL DAMP
      DO 110 I=1,NOF
  110 WRITE(6,6) FO(I),PWO(I),PW(I),ATN(I),RO1(I),ETA(I)
C
C CALCULATE  FREQUENCY PARAMETERS
      NOF=NOF-1
      WRITE(6,4)
      DO 115 I=1,NOF
      ATN(I)=(ATN(I)+ATN(I+1))/17.3717792
      F1(I)=FO(I)
      F2(I)=FO(I+1)
      FO(I)=(F1(I)+F2(I))/2.0
      DELF(I)=F2(I)-F1(I)
      WRITE(6,7) FO(I),F1(I),F2(I),DELF(I),ATN(I)
```



```
  115 CONTINUE
      DO 125 I=1,NOF
      DO 120 J=1,NOF
      Z1(I,J)=F1(I)/FO(J)
      Z2(I,J)=F2(I)/FO(J)
  120 CONTINUE
  125 CONTINUE
C
C CALL SUBROUTINE TO COMPUTE DAMPING CONSTANTS
      CALL DAMP
C COMPUTE PROPAGATION PROPERTIES FOR FREQUENCY INTERVALS
      CALL PROP
C
C INITIAL TRIAL CONCENTRATION
C
      N=NOF/2
      P=PO*100000.0
      VMIN=2.0*SQRT(P*RHO2*(RHO2-RHO1)*(CO*CO*RHO2-P))/(CO*CO*RHO2*RHO2
     1       -P*RHO1)
      P=P-PV
      CON1=XGAMA*P/(PI     *RHO2*CO)
      T=ATN(N)*XG(N)/(FO(N)**2*B1(N,N))*CON1**.5
      DO 130 I=1,NOF
      PW(I)=ATN(I)/(RHO2*CO*PI*FO(I))
      TAO(I)=T
      ATN(I)=ATN(I)*CON1       /FO(I)**2
  130 CONTINUE
      IF(ITAO) 133,134,133
  133 READ(5,14) (TAO(I),I=1,NOF)
C
C ITERATION PROCEEDURE FOR CONCENTRATIONS
C
  134 L=1
  135 WRITE(6,11) L
      DO 145 I=1,NOF
      VR(I)=0.0
      DO 140 J=1,NOF
  140 VR(I)=VR(I)+TAO(J)*A1(J,I)/XG(J)
      VR(I)=1.0/(RHO2*CO*CO)+1.0 /(XGAMA*P       )*VR(I)*FO(I)
      PWO(I)=VR(I)
      VR(I)=1.0/SQRT(RHO2/2.0*ABS(SQRT(PW(I)**2+VR(I)**2) +VR(I)))/CO
      IF(VR(I)) 144,144,145
  144 VR(I)=VMIN
  145 CONTINUE
      DO 160 K=1,NOF
      I=NOF+1-K
      F1(I)=TAO(I)
      A=TAO(I)
      TAO(I)=0.0
      B=0.0
      DO 155 J=1,NOF
  155 B=TAO(J)*B1(J,I)/XG(J) +B
      TAO(I)=(ATN(I)/VR(I)-B)/B1(I,I)*XG(I)
      PW(I)=FO(I)/(XGAMA*P)*(B+TAO(I) *B1(I,I)/XG(I))
      IF(TAO(I)) 157,157,158
  157 TAO(I)=0.0
```

```
      F1(I)=1.0
      GO TO 159
  158 F1(I)=F1(I)/TAO(I)
  159 WRITE(6,9) FO(I),VR(I),A,TAO(I),F1(I)
  160 CONTINUE
      L=L+1
      DO 180 I=1,NOF
      X=ABS(F1(I)-1.0)
      IF(X-.001) 180,180,170
  170 IF(L-61)     135,175,175
  175 WRITE(6,5) FO(I)
  180 CONTINUE
      WRITE(6,8 ) TITLE,ZA,ZB,ZC,ZD,ZE,ZF,ZG,ZH,ZI,ZJ,ZK,PO,DIST
      CT=0.0
      DO 200 I=1,NOF
      A=TAO(I)*DELF(I)
      BUB=A/(4.0/3.0*RO1(I)**3*PI)
      CT=CT+A
      WRITE(6,9) FO(I),VR(I),TAO(I),A,RO1(I),ETA(I),BUB,PWO(I),PW(I)
  200 CONTINUE
      WRITE(6,10)CT
      WRITE(6,15)SP1,XK1,YMU,RHO2,CO,XGAMA,SIGMA,PV,CON3
      IF(JOBS)100,50,100
C
C INPUT/OUTPUT CONTROL
C
    1 FORMAT(5I2)
    2 FORMAT(6F12.6)
    3 FORMAT(1H1,21X,24HBUBBLE SPECTRUM ANALYSIS,//,31X, 9HTEST DATA)
    4 FORMAT(1H2,19X,20HFREQUENCY PARAMETERS,//,7X,2HF0,10X,2HF1,10X,
     1       2HF2,8X, 7HDELTA F,3X,10HATTN NP/CM)
    5 FORMAT(1H1,21HNOT CONVERGING FOR F=,F10.1)
    6 FORMAT(F12.1,6F12.6)
    7 FORMAT(4F12.1,F12.6)
    8 FORMAT(1H1,41X,24HCOMPUTED BUBBLE SPECTRUM,//,18X,12A6,//,30X,
     1              10HP(STATIC)=,F6.4,7H ATMOS,F6.3,18H CM BETWEEN PROBES
     2      //,4X,  9HFREQUENCY,
     3       3X, 8HVELOCITY,6X,3HTAO,4X,13HCONCENTRATION,4X,4HR,CM,
     4       8X,4HDAMP,5X,9HN0 BUB/CC,7X,1HA,11X,1HB)
    9 FORMAT(F12.1,F12.6,E12.3,E12.3,F12.6,F12.6,E12.3,2E12.3)
   10 FORMAT(1H0,33X,20HTOTAL CONCENTRATION=,E11.3)
   11 FORMAT(1H2,22X,13HITERATION NO.,I2,//,3X, 9HFREQUENCY,4X,7HVR(I-1)
     1          5X, 8HTAO(I-1),5X, 6HTAO(I),6X,5HRATIO)
   12 FORMAT(12A6)
   13 FORMAT(/,15X10HP(STATIC)=,F6.4,7H ATMOS,F6.3,18H CM BETWEEN PROBES
     1       //    1X,11H  FREQUENCY,4X, 8HAMPL W/O,4X, 7HAMPL W/,4X,
     2       10HATTN DB/CM,5X,4HR,CM,8X,4HDAMP,/)
   14 FORMAT(E9.3,5E12.3)
   15 FORMAT(//,43X,18HPHYSICAL CONSTANTS,//,8X,3HSP1,9X,1HK,11X,2HMU,
     1       9X,3HRHO, 9X,1HC, 9X,5HGAMMA, 6X,5HSIGMA,9X,2HPV, 9X,4HCON3
     2       / ,4F12.6,F12.2,F12.6,F12.2,F12.6       )
   50 CONTINUE
      STOP
      END
```



```
      SUBROUTINE DAMP
      DIMENSION FO(50),F1(50),F2(50),ATN(50),Z1(50,50),Z2(50,50),
     1   B1(50,50),A1(50,50),TAO(50),VR(50),RO1(50),XG(50),ETA(50),
     2       DELF(50)
      COMMON FC,      PO,NOF,PI,RO1,XG,ETA,XGAMA,RHO2,CO,Z1,B1,A1,Z2
      COMMON      SP1,XK1,YMU,                SIGMA,PV,CON3
      CON4=3.0*XGAMA-3.0
      RHO1=CON3*PO
      CON1=RHO1*SP1*0.5/XK1
      POP=PO*1000000.0-PV
      IF(POP)  4,4,5
    4 WRITE(6,13)
      GO TO 14
    5 CON5=2.0*SIGMA/POP
      CON2=SQRT(3.0*XGAMA*POP/RHO2)
      DO 10 I=1,NOF
      WO=2.0*PI*FO(I)
      PHI=SQRT(CON1*WO)
      RO3=CON2/WO
      RO1(I)=RO3
      ALFA=1.1
      L=1
      NAP=0
    6 RO2=RO1(I)
      RO1(I)=RO3*SQRT(1.0/ALFA+CON5/RO1(I)*(1.0/ALFA-1.0/(3.0*XGAMA)))
      X=2.0*PHI*RO1(I)
      IF(X-88.0) 40,40,41
   40 DEL=COSH(X)-COS(X)
      A=SINH(X)
      A=SINH(X)
      B=SIN(X)
      DELTH=((A+B)/DEL-2.0/X)/(X/CON4+(A-B)/DEL)
      ALFA=(1.0+DELTH*DELTH)*(1.0+CON4/X*(A-B)/DEL)
      GO TO 42
   41 DELTH=(1.0-2.0/X)/(1.0+X/CON4)
      ALFA=(1.0+DELTH*DELTH)*(1.0+CON4/X)
   42 IF(NAP) 44,43,44
   43 NAP=1
      GO TO 6
   44 L=L+1
      X=ABS(RO2/RO1(I)-1.0)
      IF(X-.0001) 9,9,7
    7 IF(L-15)6,6,8
    8 WRITE(6,11)
      GO TO 10
    9 G=1.0+CON5*(1.0-ALFA/(3.0*XGAMA))/RO1(I)
      XG(I)=G/ALFA
      A=3.0*XGAMA*POP
      DELVIS=4.0*YMU/(A/XG(I))*WO
      DELRAD=SQRT(A*XG(I)/RHO2)/CO
      ETA(I)=DELTH+DELVIS+DELRAD
   10 CONTINUE
   11 FORMAT(16H2NOT CONVERGING      )
   13 FORMAT(22H2PRESSURE LESS THAN PV
   14 CONTINUE
      RETURN
      END
```

```
      SUBROUTINE PROP
      DIMENSION FO(50),F1(50),F2(50),ATN(50),Z1(50,50),Z2(50,50),
     1   B1(50,50),A1(50,50),TAO(50),VR(50),RO1(50),XG(50),ETA(50),
     2       DELF(50)
      COMMON FO,      PO,NOF,PI,RO1,XG,ETA,XGAMA,RHO2,CO,Z1,B1,A1,Z2
      COMMON      SP1,XK1,YMU1                SIGMA,PV,CON3
      DO 12 I=1,NOF
      C1=ETA(I)*ETA(I)
      C2=SQRT(4.0-C1)
      DO 12 J=1,NOF
      C3=Z2(I,J)*Z2(I,J)
      C4=Z1(I,J)*Z1(I,J)
      ADD=0.0
      DENOM=4.0*(C3-1.0)*(C4-1.0)+2.0*C1*(C4+C3)
      IF(DENOM) 2,1,3
    1 ADD=PI/2.0
      X=0.0
      GO TO 4
    2 ADD=PI
    3 X=ATAN(2.0*ETA(I)*C2*(C3-C4)/DENOM)
    4 BTM=(1.0-0.5*C1)/C2*(ADD+X)
      BTL=.25*ETA(I)*ALOG(((C3-1.0)**2+C1*C3)/((C4-1.0)**2+C1*C4))
      B1(I,J)=BTM+BTL
      C5=Z1(I,J)*Z2(I,J)
      DENOM=C5*(C5+C1)-C4-C3+1.0
      IF(DENOM) 6,5,7
    5 X=0.0
      ADD=-.5*PI
      GO TO 9
    6 ADD=-PI
      GO TO 8
    7 ADD=0.0
    8 X=ATAN(ETA(I)*(Z1(I,J)-Z2(I,J))*C5+1.0)/DENOM)
    9 ATM=0.5*ETA(I)*(ADD+X)
      A=(Z2(I,J)*(Z2(I,J)-C2)+1.0)/(Z2(I,J)*(Z2(I,J)+C2)+1.0)
      A=A*(Z1(I,J)*(Z1(I,J)+C2)+1.0)/(Z1(I,J)*(Z1(I,J)-C2)+1.0)
      ATL=(0.5-0.25*C1)/C2*ALOG(A)
      A1(I,J)=Z2(I,J)-Z1(I,J)+ATM+ATL
   12 CONTINUE
      RETURN
      END
```

APPENDIX C

ATTENUATION MEASUREMENTS IN THE NSRDC 12-INCH WATER TUNNEL

Each environment for which bubbles are to be detected should be considered separately. For example, in a towing basin, the static pressure would be between 1 and 2 atmospheres and the expected bubble radius would be in the micron range. Figure 2 indicates a resonance near 300 kHz for a 10-micron bubble. The resonance of the projecting system should be just below this value, say, 150 kHz. The bandwidth of the projector would determine the desired transducer resonance more precisely and also determine the lower limit for which signals could be propagated. Exploratory tests in metal cylinders indicated that flush mounting was undesirable because reflections were produced. Thus the mounting might be a problem in closed-jet test sections. A low mechanical Q is required for a wide-band transducer. Information on suitable properties of the transmitter is given in the book by Hueter and Bolt,[28] especially Chapters 4 and 8.

In the 12-in. open-jet tunnel, operating pressures are anticipated to average about 0.3 atmospheres. The frequency range needed to determine bubbles from 10 microns to 1 mm would be approximately 2 to 200 kHz. Preliminary investigation showed, however, that environmental noise and structures would limit the lower frequencies in the water tunnel to about 6 kHz. Measurements of the noise spectrum indicated that there was little noise above this frequency and that the path length across the open jet was sufficient to receive 1 cycle before reflections from the walls interfered with the received signal.

An investigation of available laboratory hydrophones indicated that the Atlantic Research BC-32 (an older version of the presently produced LC-32 model and one using barium titanate as the crystal element) would radiate signals of sufficient level to permit operation above 10 kHz. A combination of transducer and amplifier characteristics limited upper frequency response to 250 kHz.* In actuality, the lower limit was not met, as will be discussed later.

---

*This limit was not always possible even with the same equipment. Since at this high frequency the wavelength is about equal to transducer dimensions, the spherical wave assumption is no longer valid.

All components in the system are commercially available units which could be replaced with units of equal quality manufactured by another company. For the most part, the instrumentation used was selected because of availability rather than purchased specifically for the project.* For the transmitting system, a standard sine wave oscillator was used to generate the signal. The frequency scale on the oscillator was found to be sufficiently in error to require a digital counter to set the desired frequency. A General Radio Type 1396-A Tone Burst Generator was used to produce coherent signals of a fixed number of cycles followed by a fixed off period. Such a signal was necessary to avoid standing waves. The tone-burst wave was amplified by a McIntosh 60-w power amplifier** which drove the BC-32 transducer. The transducer was shunted with a 500-ohm, 100-w resistor (two 1000-ohm, 50-w resistors) to match the high-voltage output impedance.

The receiving portion of the instrumentation consisted of an Atlantic Research LC-5 Hydrophone*** whose signal was amplified by an Ithaco Model 252 Variable-Gain Voltage Amplifier. A 5-kHz cutoff, high-pass, active filter was used to remove the low frequency tunnel noise from the amplified signal. The filtered output was displayed on a Tektronix 561A Dual Trace Oscilloscope. The level of the received signal was measured on the oscilloscope face for each test condition.

Several aspects of the tests to be described need improvement and suggested improvements will be discussed. The tests are presented in this preliminary stage to demonstrate the feasibility of the attenuation measurements and not as data collection only.

---

*The tone burst generator is the one exception.

**This amplifier is not intended for frequencies much above 100 kHz. On several occasions, output tubes were burned out at high frequencies. Subsequent experiences with a Krohn-Hite Model DCA-50 Amplifier have been encouraging.

***Resolution (i.e., signal-to-noise ratio) could have been increased with this hydrophone by insulating the sting mount from the water since the sting is part of the circuit.

The instrumentation (Figure 11) was set up as described with hydrophones mounted on brass straps bolted to the upstream nozzle and measurements were made over a frequency range from 12.6 to 126 kHz. Frequencies much below 12.6 kHz were unusuable because at the low static pressure (when bubbles were present) the background noise contained high frequency components apparently originating from cavitation on the lip of the downstream nozzle. As can be seen from the oscilloscope traces in Figure 12, the noise is high frequency and possibly could be eliminated with a band-pass filter. Response fell off rapidly above 126 kHz and prevented data collection at the next frequency, but it was sufficient at this pressure to determine bubbles of 10 microns radius. Typically a half hour would be required to obtain data over a frequency range.

Typical oscilloscope traces are shown in Figure 12 for the lowest frequency, a mid-frequency, and the highest frequency used. The upper trace in each photograph is the tone burst before amplification, the lower is the received signal propagated through the water.

In all photographs the sweep is 50 msec per division and the vertical deflection is 0.5 v per division for the upper signal. (Signal level across the transmitting hydrophone is approximately 240 v peak to peak.) The received signal is 0.05 v per division at 12.6 kHz and 0.1 v per division at the higher frequencies. Two photographs are shown for the received signal when bubbles are present. At high pressures, the received signal is steady in time whereas at low pressure there is considerable variation in the received signal at the mid and high frequencies. Typical variations are apparent in the photographs. The distortion evident in the received signal at 62.9 kHz is caused by the large driving voltage. The distortion disappears at lower voltages ($\sim$200 v). At 62.9 and 126 kHz, the electrical pickup from the driving voltage is seen in the received signal. This is the lowest level of pickup attained and resulted from watching the grounding carefully. Isolated power supplies and monitors for the transmitting and receiving system might have done as much. Distortions in the initial and final portions of the tone burst are also evident in the photographs; these are thought to be caused by initial shock excitation and ringing, respectively.

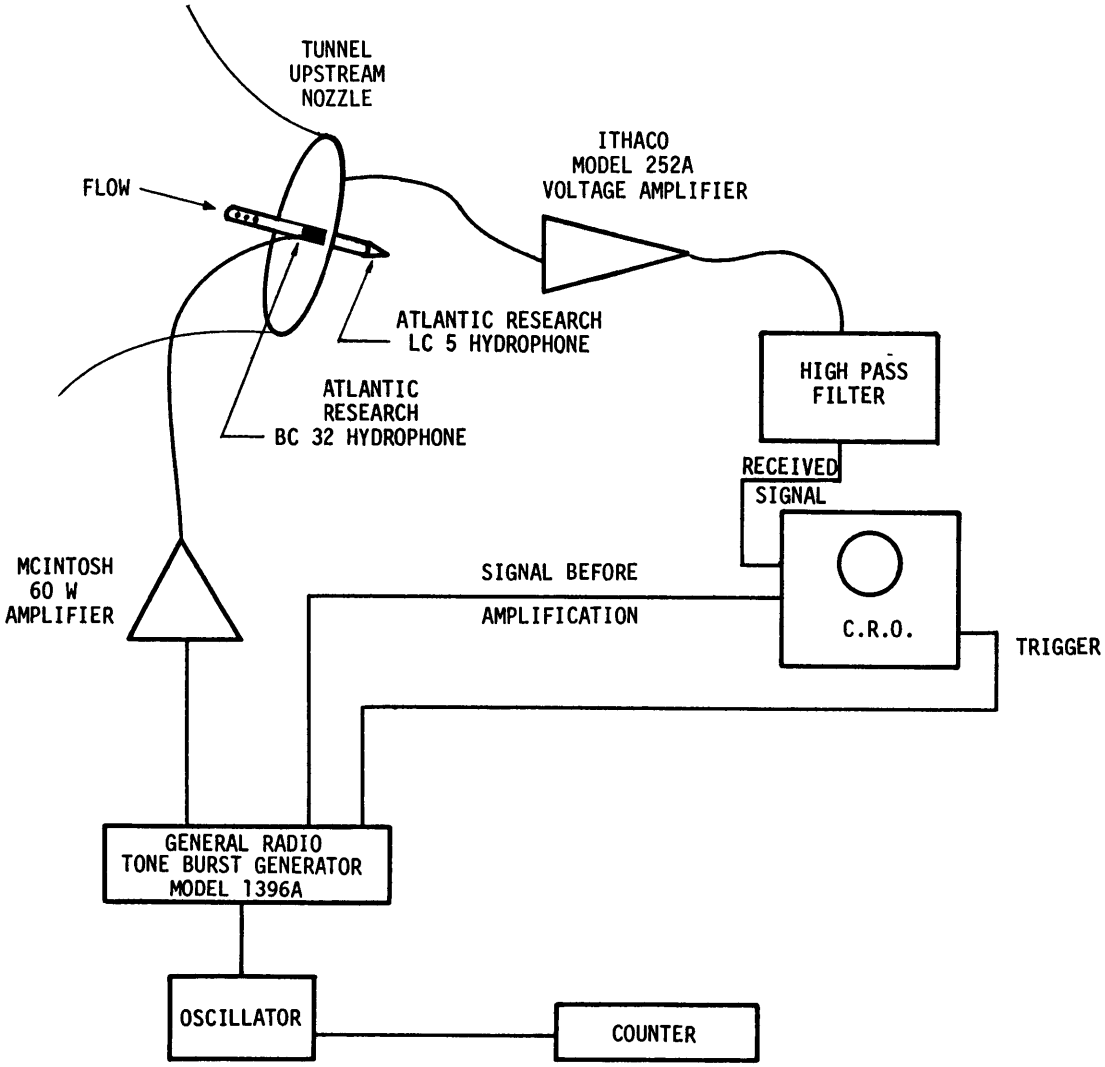

Figure 11 - Instrumentation Used to Evaluate Bubble Distribution in NSRDC 12-Inch Water Tunnel

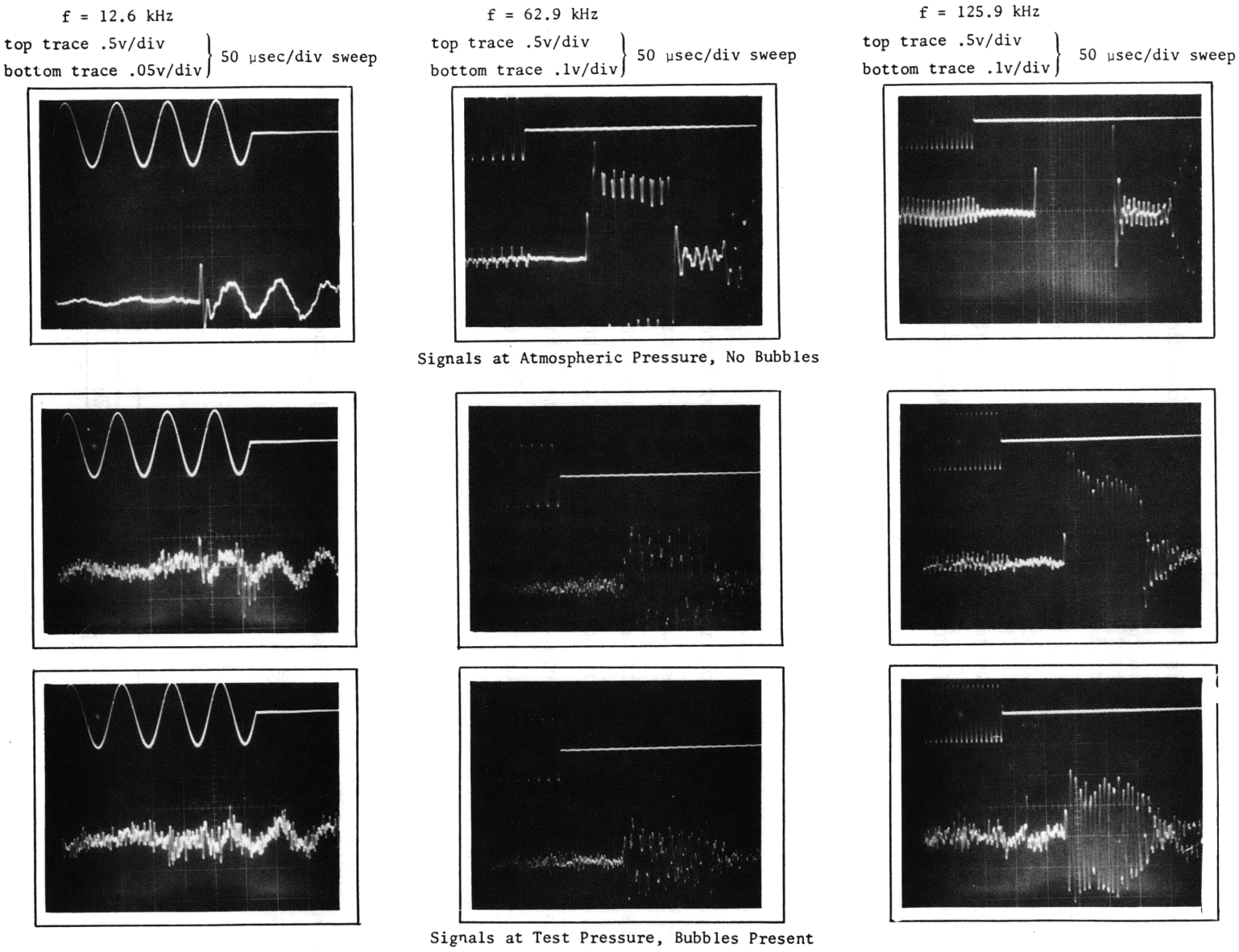

Figure 12 - Oscilloscope Traces of Received Signals with and without Bubbles in the Water

The signal level received by the LC-5 hydrophone is shown in Figure 13. The curve for the signal received with bubbles represents visually averaged values. Figure 13 also shows the ratio of the received signals and the computed bubble distribution. The presence of the three peaks in the pressure ratio was unexpected. The computed bubble spectrum smooths some of the peaks because of the averaging of attenuation in the analysis. The received signal in the first part of Figure 13 had unexpected humps and hollows but these were not considered a problem since they were present in both signals. This might arise from too high a voltage to the barium titanate transmitter, especially in view of the distortion evident in the received trace at 62.9 kHz for this driving voltage.

Another problem with the transmitting system is the steepness of the curve between 62.9 and 79.2 kHz. Since this region is not used here, it is only a potential problem. It is expected that the transmitter characteristics would be a function of temperature, time, pressure, etc. For the most part, these would produce minor effects, but the overall effect might be large in a region of steep gradient. The transmitting hydrophone intended for use in this project was not available at test time. A check of its characteristics had shown a more gradual rise in radiated pressure from low frequencies to resonance. Barium titanate has a high mechanical Q compared to other available materials. In addition, it cannot be driven at as high a voltage as can some other materials.

After the tests were completed, it was discovered that the level of signal was too high for assuming small motions. Maximum motion is expected to occur at resonance, and from Equations [17] and [14] the amplitude of oscillations for $\omega_o/\omega = 1$ is

$$\left|\frac{\Delta R}{R_o}\right| = \frac{P}{3\eta\delta\left(P_o - P_v\right)\sqrt{1 + \frac{2\sigma}{\left(P_o - P_v\right)R_o}\left(1 - \frac{1}{3\eta}\right)}}$$

where P is the amplitude of the acoustic signal. The square root term contributes about 10 percent to the right-hand side for these tests and can be

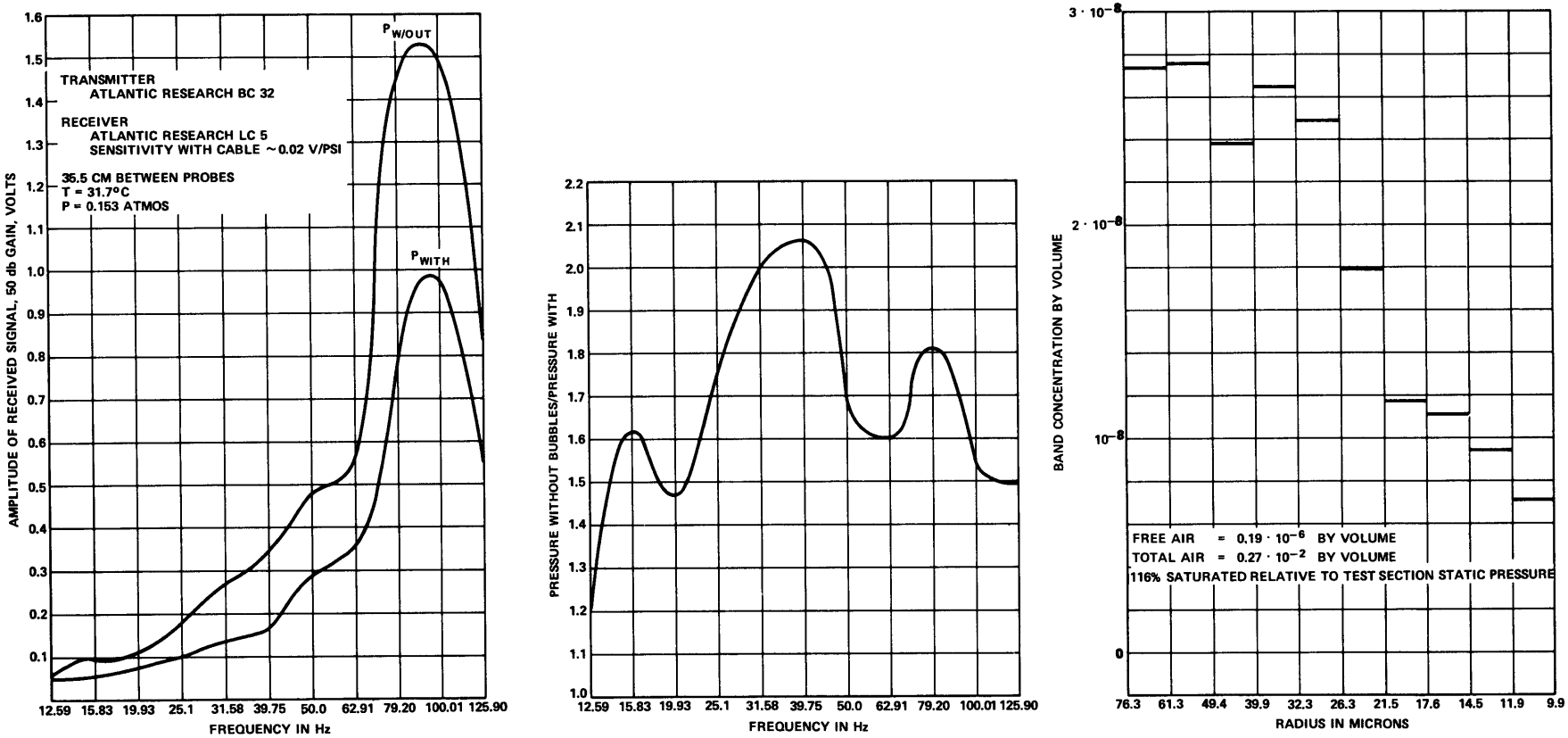

Figure 13 - Test Results and Computed Bubble Distribution

ignored. Minimum computed damping is about 0.045, $(P_o - P_v)$ is about 0.1 atmosphere, the polytropic constant is about 1 for the small bubbles here, and the maximum acoustic pressure at the receiver is about 0.01 atmosphere. Thus $\Delta R/R_o$ is approximately 0.7 and the acoustic approximation is no longer valid. A reasonable limit for the linearization approximation would be $\Delta R/R_o \leq 0.2$ for which the acoustic pressure should be $P \leq 0.6\ \delta\ (P_o - P_v)$. Effects of large amplitude motions are clouded by the unknown damping constant. If a damping constant of 0.2 were applicable, the oscillations would be marginally small in this case. Obviously higher static pressures would also permit greater acoustic signals.

Of course in this test the diving voltage could have been changed with frequency in order to keep amplitude within the limits of small motions. However the water in this test was deareated and only slightly supersaturated relative to tunnel test section pressure. Only a few tiny bubbles were visible when illuminated with stroboscopic light. Another test was attempted with the total air content (as measured with the Van Slyke apparatus) three times the saturation value relative to test section pressure. At the higher air content, bubbles were in such number as to obstruct vision. Maximum bubble size was visually estimated to be about 1 mm in diameter. For the high air content, measurable signals were recorded only above 50 kHz. At lower frequencies, the attenuation was high enough to obscure the signal. The signal received with bubbles in the water was 1/13 that at atmospheric pressure for 50 kHz, increasing to 1/3 the atmospheric value at 126 kHz. Thus large amplitude signals are needed in some situations. If the source and receiver were closer together, lower amplitude signals could be used even with large free-air contents.

To cover the low frequencies when many bubbles are present, another transmitting hydrophone should be used with a resonance in the 30-40 kHz range. The Atlantic Research LC-30 Hydrophone will be used for the low frequency region in future tests. This hydrophone crystal can be excited with up to 500 v and has a broader range than the BC-32 hydrophone.

REFERENCES

1. Bernd, L., "Cavitation, Tensile Strength and the Surface Films of Gas Nuclei," Sixth Naval Hydrodynamics Symposium, ONR, Washington, D.C. (Sep 28 - Oct 4 1966).

2. Hsieh, T., "The Influence of the Trajectories and Radial Dynamics of Entrained Gas Bubbles on Cavitation Inception," Hydronautics, Inc., Technical Report 707-1 (Oct 1967).

3. Holl, J.W. and Treaster, A.L., "Cavitation Hysteresis," Transactions of the American Society of Mechanical Engineers, Vol. 88, Series D, No. 1, pp. 199-212 (1966).

4. Peterson, F.B., "Cavitation Originating at Liquid-Solid Interfaces," NSRDC Report 2799 (Sep 1968).

5. Iyengar, K.S. and Richardson, E.G., "Measurements of the Air-Nuclei in Natural Water Which Give Rise to Cavitation," British Journal of Applied Physics, Vol. 9, pp. 154-158 (Apr 1958).

6. Thompson, B.J. et al., "Application of Hologram Techniques for Particle Size Analysis," Applied Optics, Vol. 6, No. 3, pp. 519-526 (1967).

7. Ellis, A.T., "Parameters Affecting Cavitation and Some New Methods for Their Study," California Institute of Technology Hydrodynamics Laboratory Report E-115.1 (Oct 1965).

8. Fox, F.E. et al., "Phase Velocity and Absorption Measurements in Water Containing Air Bubbles," Journal of the Acoustical Society of America, Vol. 27, No. 3, pp. 534-539 (1955).

9. Strasberg, M., "Onset of Ultrasonic Cavitation in Tap Water," Journal of the Acoustical Society of America, Vol. 31, pp. 163-176 (1959).

10. Buxcey, S. et al., "Acoustic Detection of Microbubbles and Particulate Matter Near the Sea Surface," Masters Thesis, U.S. Naval Postgraduate School, Monterey, California (1965).

11. Smith, H.D. Jr. and Pipkin, E.L., "Acoustic Determination of a Bubble Size Distribution," U.S. Navy Mine Defense Laboratory, Report 286 (Feb 1966).

12. Killen, J.M. and Ripkin, J.F., "A Water Tunnel Air Content Meter," Saint Anthony Falls Hydraulic Laboratory Project Report 70 (Feb 1964).

13. Meyer, E. and Skudrzyk, E., "On the Acoustical Properties of Gas Bubble Screens in Water," (in German) Acustica, Vol. 3, pp. 434-440 (1953); also NSRDC Translation 285 (Nov 1958).

14. Spitzer, L., Jr., "Acoustic Properties of Gas Bubbles in a Liquid," Office of Scientific Research and Development, National Defense Research Committee, Division 6 - Section 6.1, OSRD No. 1705, Section No. 6.1 - sr 20-918 (Jul 1943).

15. Carstensen, E.L., and Foldy, L.L., "Propagation of Sound through a Liquid Containing Bubbles," Journal of the Acoustical Society of America, Vol. 19, pp. 481-501 (1947).

16. Chow, J.C.F., "The Attenuation of Acoustic Waves in a Two Phase Medium," Division of Engineering, Brown University, ABL/X96 (May 1963).

17. Hsieh, D.Y. and Plesset, M.S., "Theory of the Acoustic Absorption by a Gas Bubble in a Liquid," California Institute of Technology, Engineering Division, Report 85-19 (Nov 1961).

18. Devin, C., Jr., "Survey of Thermal, Radiation, and Viscous Damping of Pulsating Air Bubbles in Water," Journal of the Acoustical Society of America, Vol. 31, pp. 1654-1667 (1959); also NSRDC Report 1329 (Aug 1959).

19. Lamb, H., Hydrodynamics, Dover (1932).

20. Turner, W.R., "Physics of Microbubbles," Vitro Laboratories Technical Note 01654.01-2 (Aug 1963).

21. Wadmark, B., "Some Aspects of the Measuring of Free Gas Bubbles in Water with Special Attention to the Measurement of the Speed of Sound," The Swedish State Shipbuilding Experimental Tank, PM K54-6A (Mar 1968).

22. Ripkin, J.F., "A Study of the Influence of Gas Nuclei on Cavitation Scale Effects in Water-Tunnel Tests," Saint Anthony Falls Hydraulic Laboratory Project Report 58 (Feb 1958).

23. Exner, M.L. and Hampe, W., "Experimental Determination of the Damping of Pulsating Air Bubbles in Water," Acustica, Vol. 3, pp. 67-72 (1953).

24. Victor, A.S., "A Study of the Damping and Stability of a Pulsating Spherical Bubble in a Flowing Fluid," Navy Mine Defense Laboratory, Report 329 (Apr 1967).

25. Strasberg, M., Letter to the editor, Acustica, Vol. 4, p. 518 (1954).

26. Strasberg, M., "The Pulsation Frequency of Nonspherical Gas Bubbles in Liquids," Journal of the Acoustical Society of America, Vol. 25, No. 3, pp. 536-537 (1953).

27. Meyer, E. and Tamm, K., "Natural Vibration and Damping of Gas Bubbles in Liquids," (in German), Akustiche Zeitschrift, Vol. 4, No. 3, (1939); also NSRDC Translation 109 (Apr 1943).

28. Hueter, T.F. and Bolt, R.H., Sonics, Wiley and Sons (1955).

INITIAL DISTRIBUTION

Copies	
4	NAVSHIPS 3 SHIPS 2052 1 SHIPS 033
6	NAVSEC 1 SEC 6100 2 SEC 6110 1 SEC 6144 2 SEC 6148
1	NAVORDSYSCOM (ORD 05411)
3	NAVAIRSYSCOM 2 AIR 604 1 AIR 302
3	CHONR 2 Code 438 1 Code 492
1	NWC, Pasadena
1	NWC, China Lake
1	CDR, USNOL
1	DIR, USNRL
1	ONR, SAN FRAN
1	CO, ONR, BSN
1	CO, ONR, Pasadena
1	CO, ONR, Chicago
25	CO, ONR, London
1	NAVSHIPYD PTSMH
1	NAVSHIPYD BSN
1	NAVSHIPYD BREM
1	NAVSHIPYD PHILA
1	NAVSHIPYD CHASN
1	NAVSHIPYD LBEACH
1	Commander, NWL Attn: Computation & Exterior Ballistics Lab
1	CO, USNROTC & NAVADMINUMIT
1	Superintendent, USNA
1	USNASL, Attn: Lib
1	CO, USNAVUWRES, Attn: Lib

Copies	
1	CO, USNEL, Attn: Lib
1	CO & DIR, USNAVCIVENGRLAB
1	NNS&DD, Engr Tech Dept
1	USNAVPGSCOL, Monterey
20	DDC
2	NASA 1 Attn: Dr. W.L. Haberman (Code MTY) 1 Attn: Dir of Research (Code RR)
2	ADMIN, MARAD 1 Attn: Ship Div 1 Attn: Coordinator of Research
1	CO, MSTS
1	BUSTAND, Attn: Lib
1	Lib of Congress, Washington
1	SUPT, USMMA
1	Commandant, USCOGARD Attn: Ship Construction Committee
1	Commander, U.S. Army Transportation Res & Dev, Fort Eustis, Va Attn: Marine Transportation Div
1	Air Force Office of Sci Res, Washington, Attn: Mech Div
1	W-PAFB, Dayton Attn: Wright Air Dev Div, Aircraft Lab
2	Langley Res Center, Langley Station, Hampton, Va 1 Attn: Mr. I.E. Garrick 1 Attn: Mr. D.J. Marten
1	DIR, Nat'l Sci Foundation, Washington, Attn: Engr Sci Div
1	Chief of Res & Dev, Office of Chief of Staff, Dept of the Army, The Pentagon

Copies	
1	DIR, WHOI
1	NASA, College Park Attn: Sci & Techn Info, Acquisitions Br
1	Commander General, Army Eng Res & Dev Lab, Fort Belvoir, Va, Attn: Techn Documents Cen
1	DIR, ORL, Penn State
1	Head, Dept NAME, MIT
4	CIT 1 Attn: Lib 1 Attn: Prof Acosta 1 Attn: Prof Plesset 1 Attn: Prof Wu
1	DIR, St. Anthony Falls Hydra Lab, Univ of Minnesota, Minneapolis
1	Univ of Notre Dame, Dept of Mech Eng, South Bend
1	DIR, Inst of Hydraulic Res, Univ of Iowa, Iowa City
1	Univ of Michigan, Dept NAME, Ann Arbor
1	Webb Inst of Nav Arch, Glen Cove 1 Attn: Lib
2	Univ of Calif, Berkeley 1 Attn: Lib 1 Attn: Head, Dept NAVARCH
2	State Univ of Colorado, Fort Collins, Colorado 1 Attn: Dr. M.L. Albertson 1 Attn: Prof J.E. Germak
1	Cornell Univ, Graduate School of Aeronautical Eng, Ithaca
1	Harvard Univ, Cambridge Attn: Lib
2	JHU, Baltimore 1 Attn: Dept of Mechanics 1 Attn: Inst of Cooperative Res

Copies	
2	State Univ of New York, Maritime College, Bronx, N.Y. 1 Attn: Engr Dept 1 Attn: Inst of Math Sci
1	Princeton Univ, Princeton, N.J. Attn: Lib
1	Stanford Univ, Stanford, Calif Attn: Dept of Civil Eng
1	Univ of Illinois, Dept of Theoretical & Applied Mech, Urbana
1	JHU, Fenton Kennedy Document Center, Applied Physics Lab, Silver Spring
1	Cornell Aeronautical Lab, Buffalo
2	Davidson Lab, SIT, Hoboken 1 Attn: Director 1 Attn: Dr. Tsakonas
1	Rensselaer Polytechnic Inst, Dept of Mathe, Troy, N.Y.
1	Puget Sound Bridge & Drydock Co, Seattle
1	Douglas Aircraft Co, General Applied Sci Lab, Westbury, L.I., N.Y.
1	ITEK Corp, Vidya Div, Palo Alto
1	TRG Inc, Melville, N.Y.
1	Therm Inc.
1	Lockheed Missiles & Space, Sunnyvale, Attn: Dept 5701
1	Lockheed Missiles & Space, Palo Alto, Attn: Tech Info Cen
1	Electric Boat Co, General Dynamics Corp, Groton
1	Robert Taggart Inc, Fairfax, Va
1	Oceanics
1	Gibbs & Cox
1	George G. Sharp, Inc.
1	Grumman Aircraft Corp., Bethpage

Copies	
1	Hydronautics, Inc.
1	Martin Co, Baltimore
1	Boeing Aircraft, AMS Div, Seattle
1	United Aircraft, Hamilton Standard Div, Windsor Locks, Conn
1	AVCO, Lycoming Div, Washington
1	Baker Mfg, Evansville
2	General Dynamics - Convair, San Diego 1 Attn: Dr. B.R. Perkin 1 Attn: Chief of ASW/Marine Sci
1	Curtiss-Wright Corp, Woodridge, N.J.
1	FMC
1	President, General Technical Services, Inc, Cleveland
1	Dr. S.F. Hoerner, 148 Busteed Drive, Midland Park, N.J.
1	RCA, Burlington, Mass Attn: Hydrofoil Projects
1	U.S. Rubber Co, Res & Dev Dept, Wayne, N.J.
1	Midwest Research Inst, Kansas City, Mo Attn: Lib
1	North American Aviation Inc, Oceans Systems Div, Downey, Calif
1	Aerojet-General Corp, Azusa
1	SNAME
1	ASNE, Washington
1	ASME, Res Comm in Information, New York
1	Inst of Aerospace Sciences, New York Attn: Lib

UNCLASSIFIED

Security Classification

DOCUMENT CONTROL DATA - R & D

(Security classification of title, body of abstract and indexing annotation must be entered when the overall report is classified)

1. ORIGINATING ACTIVITY (Corporate author)	2a. REPORT SECURITY CLASSIFICATION
Naval Ship Research and Development Center Washington, D.C. 20007	Unclassified
	2b. GROUP

3 REPORT TITLE

COMPUTATIONAL METHOD FOR DETERMINATION OF BUBBLE DISTRIBUTIONS IN LIQUIDS (U)

4 DESCRIPTIVE NOTES *(Type of report and inclusive dates)*

Final Report

5. AUTHOR(S) *(First name, middle initial, last name)*

Terry Brockett

6. REPORT DATE	7a. TOTAL NO. OF PAGES	7b. NO. OF REFS
April 1969	69	28

8a. CONTRACT OR GRANT NO.	9a. ORIGINATOR'S REPORT NUMBER(S)
b. PROJECT NO. S-R009 01 01	2798
c. Task 0101	9b. OTHER REPORT NO(S) *(Any other numbers that may be assigned this report)*
d.	

10. DISTRIBUTION STATEMENT

This document has been approved for public release and sale; its distribution is unlimited.

11. SUPPLEMENTARY NOTES	12. SPONSORING MILITARY ACTIVITY
	Naval Ship Research and Development Center

13. ABSTRACT

An analytical method of determining the gas bubble spectrum in a liquid from the measured acoustic attenuation is examined. The analysis is based on the linearized equations of motion for a spherical bubble with damping. The bubbles are assumed to be homogeneously distributed in the liquid and the bubble concentration and damping are assumed constant in a small size interval. The acoustic wavelength is assumed much greater than the bubble dimensions and bubbles are assumed far enough apart that no interactions occur. The direct solution gives the acoustic attenuation of a known bubble distribution at any given frequency. An iteration precedure is incorporated in a FORTRAN program for converting acoustic attenuation as a function of frequency to bubble concentration as a function of size. For air bubbles in water, the effects of physical properties on the bubble spectrum are examined with the computer program. Experiments in the 12-inch water tunnel are described.

14. KEY WORDS	LINK A		LINK B		LINK C	
	ROLE	WT	ROLE	WT	ROLE	WT
Gas Bubble						
Nuclei Distribution						
Acoustic Attenuation						
Acoustic Propagation						
Cavitation						